DESK COPY

Fracture distribution in faulted basement blocks: Gulf of Suez, Egypt

AMGAD I. YOUNES[1,*], TERRY ENGELDER[1] & WILLIAM BOSWORTH[2]

[1]*Department of Geosciences, The Pennsylvania State University, University Park, PA 16802, USA*

[2]*Marathon Petroleum Egypt Ltd, PO Box 52, Maadi, Cairo, Egypt*

Abstract: Fractures in basement rocks of Gebel El Zeit and Esh El Mallaha fault blocks, Egypt, occur in three nearly orthogonal sets: a SE-dipping, cross-rift set that parallels ENE faults and dykes; a SW-dipping set sub-parallel to bedding in overlying clastic rocks; and a NE-dipping, rift-parallel set that parallels the rift-border faults. Restoration to pre-rift orientations puts these sets into vertical, horizontal and vertical attitudes respectively. All fracture sets are present throughout the fault blocks, except for the horizontal set which is absent on the NE side of Gebel El Zeit and in the Nubia Sandstone. Fracture density increases near the top of basement where sheet fracturing is common, near faults, and in and around dykes. The distribution of similar fracture sets is recorded from sub-surface Formation Micro Scanner and Formation Micro Imager logs in the basement of the Ashrafi Oil-field, southern Gulf of Suez. The similarity of the fracture pattern between Gebel El Zeit and the Ashrafi Field suggests that surface fault blocks can be adequate analogues to the sub-surface blocks.

The intersection of sheet and fault-parallel fractures localizes the maximum fracture density at the edges and near the top of the fault blocks. Block faulting and subsequent depth of erosion govern the distribution of fractures within the blocks. Block rotation during rifting relocated the maximum fracture density at an upper corner or structural crest, whereas block faulting without rotation maintained the maximum fracture density at block edges. In both styles, erosion of an exhumed block removed rocks of high fracture density by eroding the crest in the first case, and by stripping off the sheet fractures in the second. The first style is an analogue for half-graben reservoirs, e.g. the southern Gulf of Suez, while the second style is an analogue for full-graben reservoirs, e.g. the Mekong Basin, southern Vietnam.

Fractured basement reservoirs are promising yet challenging targets for oil exploration and production. Recent discoveries such as the Zeit Bay and Ashrafi Fields in the Gulf of Suez, Egypt, are basement reservoirs that yield as much as 25 000 barrels of oil per day (BOPD). Other promising plays of this type are found in offshore southern Vietnam where the oil column reaches over 3000 feet high in two fields, the White Tiger and Big Bear (Chan *et al.* 1994; Arechev *et al.* 1992). One of the first steps associated with drilling and evaluating fractured basement reservoirs is to define the fracture network since it controls both porosity and permeability. Fractured granite, for example, has a bulk permeability that generally exceeds its intrinsic permeability by several orders of magnitude (Heath 1985; Freeze and Chenry 1987). Hence, data on the location and density of fractures become essential for evaluation of porosity and hydraulic parameters of a basement reservoir.

Although several borehole logging tools (e.g. Formation Micro Scanner (developed by Schlumberger), Fracture Identification Log, and BoreHole TeleViewer (developed by Schlumberger and Mobil) can detect fracture attitude and spacing, other fracture characterization parameters, such as fracture size, are difficult to judge from these tools. In order to construct a set of rules that constrain the extent and geometric relationship among different fracture sets, the reservoir engineer may resort to direct observations in outcrop. Extrapolation of surface fracture data to the sub-surface requires knowledge of how the fracture density and development are affected by differences in fault-block size, attitude, rotation, and depth of erosion.

This study focuses on some of the factors that influence the fracture density in a faulted basement block in Egypt, the Gebel El Zeit block. This rotated fault block along the western side of the Gulf of Suez was selected for its proximity to the offshore Ashrafi Field which is an oil reservoir in fractured basement (Fig. 1). First, we introduce the study area and present fracture data. Then, we present two models for fracture

* Present address: Royal Holloway College, University of London, Department of Geology, Egham, Surrey, TW20 0EX, UK

YOUNES, A. I., ENGELDER, T. & BOSWORTH, W. 1998. Fracture distribution in faulted basement blocks: Gulf of Suez, Egypt. *In*: COWARD, M. P., DALTABAN, T. S. & JOHNSON, H. (eds) *Structural Geology in Reservoir Characterization*. Geological Society, London, Special Publications, **127**, 167–190.

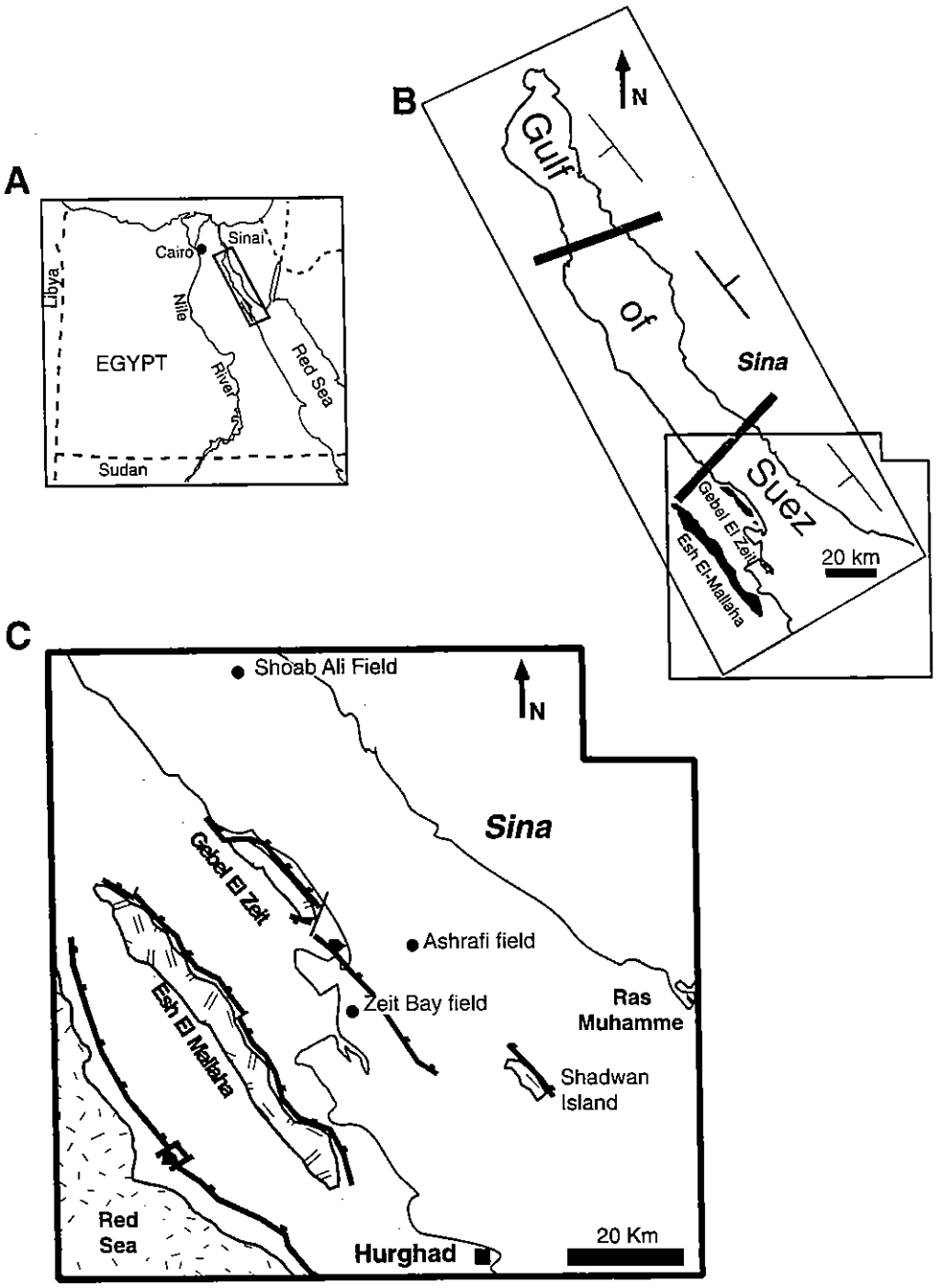

Fig. 1. (**A**) Location map of the study area. (**B**) The Gulf of Suez is divided into three half grabens (dip symbols) separated by large transverse fault zones (stripes). (**C**) The Gebel El Zeit and Esh El Mallaha fault blocks have rotated along faults that dip to the northeast (hachuring is on the downthrown side) exposing basement rocks in the core of the fault blocks (double-line hachuring). At the Gebel El Zeit block, overlying sedimentary cover dips 42° to the southwest at its contact with the basement (see Fig. 5 for detailed map). The Esh El Mallaha block dips only 7–8° to the southwest. The Shoab Ali, Ashrafi and Zeit Bay Fields produce from fractured basement reservoirs.

distribution in faulted basement blocks. We correlate the first model with a sub-surface example, the Ashrafi Field, Egypt, and then suggest a possible sub-surface analogue for the second. Finally, we discuss the significance of the fracture distribution on basement-rock permeability and reservoir potential.

Throughout the paper we use the term 'fault' to indicate a discontinuity along which significant motion (>0.5 m) took place and/or fault

surface structures are observed (Petit 1987). We use the term 'fracture' to indicate a discontinuity where displacement was not observed and thus the discontinuity can be a joint or faulted joint. A 'joint' is a fracture that opened perpendicular to a discontinuity plane and remained open (Engelder 1982). We refer to fracture rather than joint since the long history of the basement, including multiple rifting and peneplanation, makes it inevitable that some joints have slipped and become faults. Thus, it is difficult to discriminate between a reactivated joint and a discontinuity that started as a fault. Fracture orientations were measured using the right-hand rule.

Geological setting

The Gulf of Suez is a continental rift that extends for 325 km, with a maximum width of 90 km at the northern terminus of the Red Sea. Extension commenced at the southern end of the rift during the lower Miocene. There is a progressive decrease in total extension both towards the north and away from the rift axis. Shoulders of the rift extend into the African continent and are manifest as a series of rift-parallel faults along which several blocks rotated up to 45°, exposing basement-cored fault blocks such as the Gebel El Zeit and Esh El Mallaha fault blocks (Fig. 1).

Basement rocks of the Gebel El Zeit block consist of multiple intrusions of granitic to granodioritic rocks known as the Younger Granite (pink) and the Older Granite (grey), both of which were emplaced during the Precambrian cratonization of the Arabo-Nubian shield (Patton *et al.* 1994; Stern & Hedge 1985). The Older Granite (610–670 Ma) is a calc-alkaline, orogenic, mesozonal type that may be related to subduction (Stern *et al.* 1984). Conversely, the Younger Granite represents an anorogenic epizonal type that is related to a magmatic pulse associated with Cambrian rifting (Greenberg 1981). Isotope age dates from the basement exposed along the western side of the Gulf of Suez range between 620 and 570 Ma (Patton *et al.* 1994; Stern & Menton 1987; Stern & Hedge 1985; Stern *et al.* 1984; Greenberg 1981). Except for a few Cretaceous granite plutons surrounding Esh El Mallaha (Stern 1995, pers. comm.), no age dates are available for the Esh El Mallaha granite intrusion. However, because this granite intrudes late Proterozoic volcanic rocks, its age is late Proterozoic or younger. Following cratonization, the basement complex was affected by NNW extension as manifested by the formation of a series of ENE-oriented longitudinal basins in northeastern Egypt, and the simultaneous emplacement of dykes. Dykes occur in swarms oriented ENE with minor populations oriented N–S and WNW (Schurmann 1966), and show a bimodal composition that varies from rhyolite and andesite, to basalt with several textures. In Gebel El Zeit, the ENE dykes are mainly andesitic while those at Esh El Mallaha are mainly rhyolitic and are much less frequent in occurrence.

The age and depositional history of the units directly overlying the basement rocks at Gebel El Zeit are controversial (Fig. 2). For example, the age of the Nubia Sandstone varies from Cambrian or Permian (Perry 1983; Bhattacharyya & Dunn 1986; Allam 1988; Klitzsch & Squyres 1990), to early Cretaceous (Prat *et al.* 1986; Colletta *et al.* 1986). Nevertheless, after an early phase of WNW extension with ENE basement rifting, the area was exposed to erosion for long periods followed by the deposition of up to 350 m of Nubia Sandstone. The Nubia Sandstone is overlain by a sequence of marls, shales and fine sands that mark the onset of the mid-Cretaceous transgression. Miocene sediments unconformably overlie the Cretaceous section and are divided into two distinct groups: a lower Miocene clastic series that

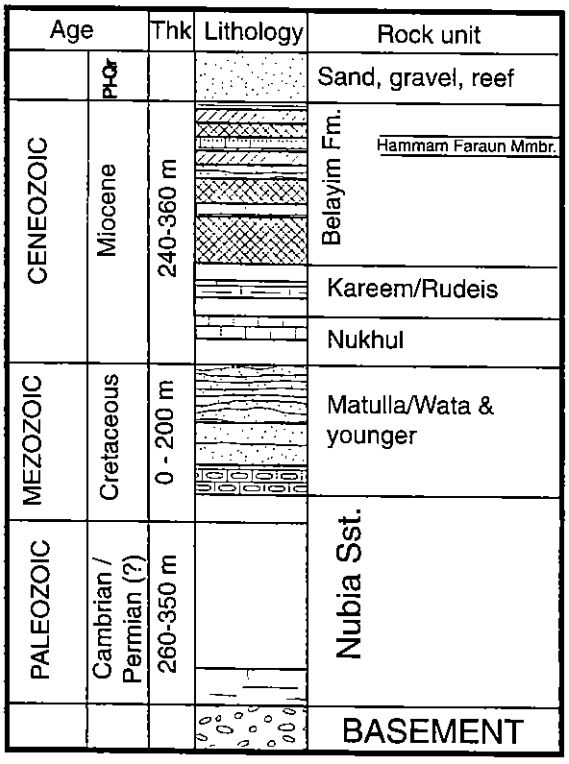

Fig. 2. Stratigraphic column of Gebel EL Zeit measured at the northern end of Wadi Kabrit.

marks the initiation of rifting (Nukhul, Rudeis and Kareem), and a middle to upper Miocene thick cover of evaporites, representing the post-rifting closure and abandonment.

The Miocene Gulf of Suez rift basin is bounded by two fault sets: a rift-parallel set (310–330°) and a cross-rift set (055–065°). The first set forms oblique- and dip-slip normal faults that are related to block rotation during the rifting of the Gulf of Suez. A left-lateral sense of slip is often recorded in the outcrop, and large ENE faults have a right-stepping arrangement (Bosworth 1995). These two fault sets divide the rift basin into a series of rotated blocks with variable sizes. Two large fault zones transect the Gulf of Suez dividing the rift basin into three dip domains (Moustafa 1976) (Fig. 1). The southern zone passes to the north of Gebel El Zeit, separating it from the structurally distinct area further north where kilometre-scale folds and greater deformation exist. Dyke swarms in the southern Gulf of Suez strike almost parallel to the previous zone. Except for syn-sedimentary folds and minor folds associated with strike-slip motion on ENE faults, no evidence for pervasive folding was observed, and has not been reported in the literature of the Gebel El Zeit area.

Although rotation of both the Gebel El Zeit and Esh El Mallaha blocks is a manifestation of the Gulf of Suez rifting, the timing and rates of exhumation of these blocks are significantly different. Apatite fission tracks show that basement rocks of the Gebel El Zeit block were at least 2–3 km deep during the early Carboniferous whereas rocks of Esh El Mallaha were at the same depth as late as the early Jurassic (Omar *et al.* 1989). The age difference implies that the onset of exhumation at Gebel El Zeit predates that at Esh El Mallaha. Therefore, if rocks of both fault blocks are of the same age, then the amount of uplift and erosion will be considerably different. Most of the present-day relief on the western margin of the Gulf of Suez is due to early Miocene rifting, at approximately 20 Ma (Omar *et al.* 1989).

Data from oil and gas exploration in the Gulf of Suez constrain the rift's structural and stratigraphic styles. A few papers (e.g. El-Shazly *et al.* 1979; Huang & Angelier 1985; Zahran & Ismail 1986) discuss the characteristics and general statistics of fractures around the Gebel El Zeit area. Recently, the discovery of hydrocarbon within fractured basement and the advance of high-resolution resistivity tools that can detect fractures in a borehole has stimulated interest in analysis of fractured basement rock.

Fractured basement of the Gebel El Zeit and Esh El Mallaha fault blocks

The basement rocks of the Gebel El Zeit block were fractured intensely during the ENE (Cambrian) and the NW (Miocene) rifting events (Husseini 1988), and systematic fracture sets were developed approximately parallel to dykes and faults associated with rifting. During rotation accompanying the Miocene rifting event, the Gebel El Zeit and Esh El Mallaha fault blocks tilted to the west by 42° and 8°, respectively. The fault slip and rotation of the Gebel El Zeit block contributed $\geq$9 km to the 35 km total extension of the Southern Gulf of Suez, whereas the rotation of Esh El Mallaha lead to $\leq$2 km of extension (Bosworth 1995). The different amounts of extension are reflected in the intensity of fracturing and faulting within the Gebel El Zeit and Esh El Mallaha fault blocks.

In the Gebel El Zeit and Esh El Mallaha blocks, fractures occur in different sets and may have different origins. Identifying the origin of a fracture set largely relies on its pervasiveness, persistence, and orientation relative to larger structures. In this paper, we are concerned only with systematic fracture sets, that is, groups of fractures that are persistent in attitude and character over large areas.

Joint sets typically form as vertical or horizontal discontinuities. Rotation of a fault block will cause a reorientation of joints so that dip changes from a minimum of 0° if joints are perpendicular to the rotation axis, to a maximum equal to the block rotation if joints are parallel to the rotation axis. Joints, or fractures, that are oriented obliquely to the rotation axis will change attitude (strike and dip) by an amount directly proportional to the amount of rotation and the angle between the rotation axis and the fracture strike. The block rotation of the Gebel El Zeit (42°) and Esh El Mallaha (8°) fault blocks illustrates this effect. In the Gebel El Zeit block, three nearly orthogonal fracture sets exist, two of which are affected by block rotation: the first, sheet fractures, show a maximum tilt equivalent to the dip of the overlying Nubia Sandstone beds (42°–45° SW); and the second, a rift-parallel set, dips 69° NE and shows less tilt because it strikes 15°–30° west of the rotation axis (Fig. 3). Only the set that is perpendicular to the rotation axis (and the rift), the cross-rift set, remains sub-vertical, dipping approximately 80° SE (this cross-rift set constitutes the face of outcrop in Fig. 3). In the Esh El Mallaha block, where rotation is only 7–10°, the sheet fracture set retains a sub-horizontal attitude

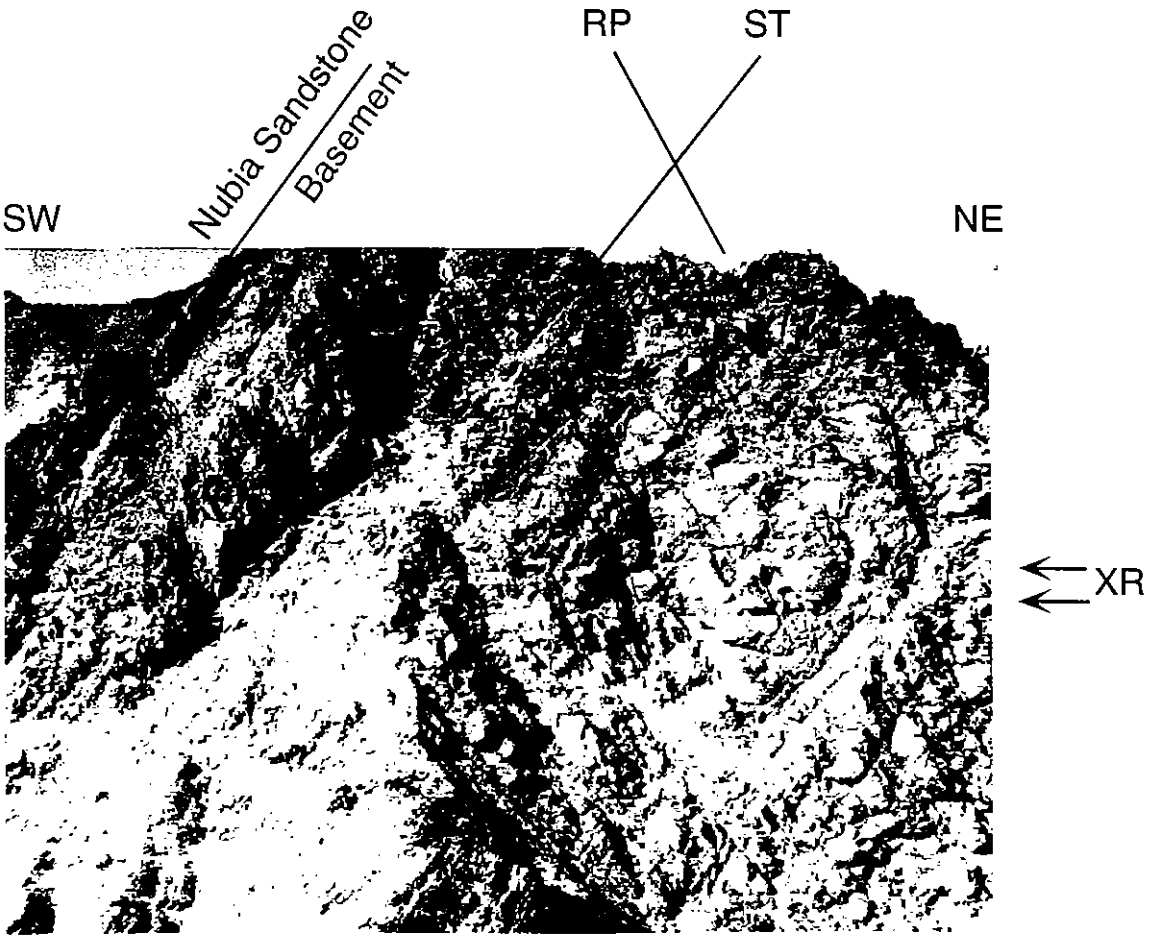

Fig. 3. Photograph showing the three mutually perpendicular fracture sets near the entrance of Wadi Kabrit, Gulf of Suez, looking NW. The sedimentary cover is exposed on the upper left corner of the photograph and dips 42° to the SW. Notice the gradual decrease in fracture density of the bedding- parallel set towards the NE. XR = cross-rift set dipping SE. ST = SW-dipping fracture set. RP = rift-parallel NE-dipping fracture set. The field of view is approximately 35 × 20 m.

and rift-parallel and cross-rift retain vertical to sub-vertical attitudes in agreement with the small rotation amount (Fig. 4).

In addition to the change of attitude by rotation, fractures in the Gebel El Zeit block differ from those at Esh El Mallaha in other aspects. For example, in the Gebel El Zeit block, the cross-rift fractures are the best developed (uniform and persistent), extending up to 15 m in length, and are distinguished by a chlorite coating on fracture walls. The rift-parallel set is less developed and is frequently found as zones lined with vug-filling quartz.

In contrast to the Gebel El Zeit block, cross-rift fractures in the Esh El Mallaha block are less developed whereas rift-parallel fractures are the best developed showing plumose structures, no fill, and reaching several tens of metres in length (Fig. 4). The sheet fractures can reach over 50 m in length, cut other fractures, and are well-developed just below the base of the Nubia Sandstone (Fig. 3). In the Gebel El Zeit block, the sheet fractures occasionally have a few pockets of vug-filling quartz, slickensides and other fracture-surface structures. On a mesoscopic scale, sheet fractures appear as planar, narrowly spaced fracture zones approximately 10–30 cm thick. The abutting relationships indicate that the rift-parallel set is younger than the sheet and cross-rift sets. The abutting relationship between the cross-rift and sheet fractures is not clear. The youngest set oriented

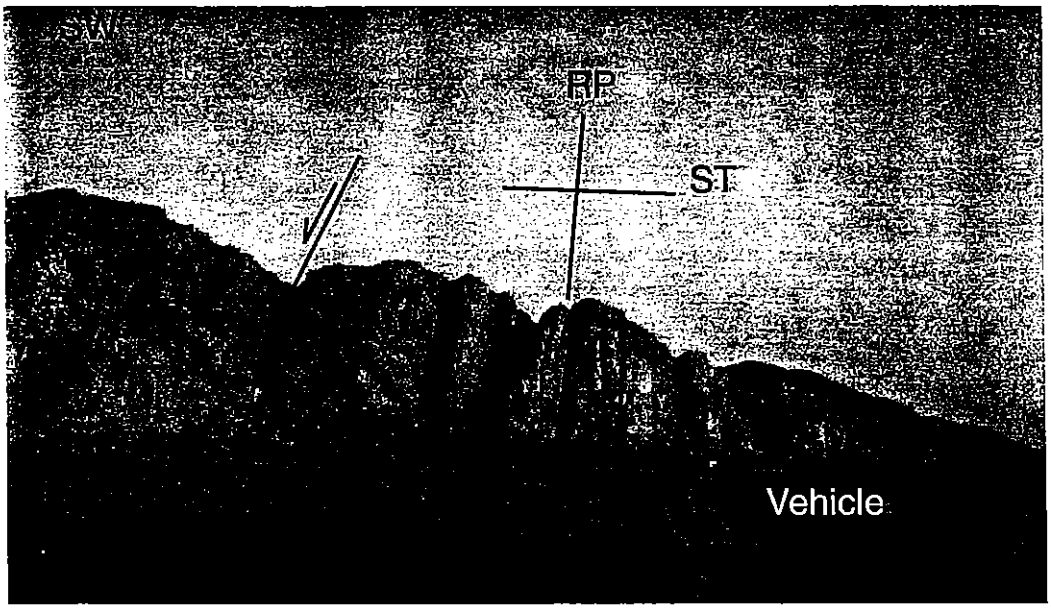

Fig. 4. Photograph of fractures in Esh El Mallaha granite. The large fracture sets are approximately 100 m high, a few metres wide, and trend NW, parallel to the Gulf of Suez. RP = rift-parallel fractures, ST = sheet fractures. Half-arrow indicates the downthrown side of a rift-parallel normal fault. Car is approximately 40 m from outcrop.

NNE has a vector mean strike at 025° and is best developed within the Esh El Mallaha block, but frequently occurs in the Gebel El Zeit block as well. The age relationships of fractures, absolute ages of basement and significance for the structural evolution of the southern Gulf of Suez will be discussed elsewhere.

Field data

Orientation, and other parameters (e.g. spacing, height, length and termination), from over 3000 fractures were systematically measured along scanlines on the eastern and western sides of the Gebel El Zeit fault block (Fig. 5). Lack of pavements on which joints are exposed and inaccessibility of outcrop faces limited our data collection to scanline surveys. Fracture orientation data from the NE side, the SW side, the Nubia Sandstone of the Gebel El Zeit, and the Esh El Mallaha fault blocks are plotted on lower-hemisphere equal-area stereonets as poles to fractures (Fig. 6). On the SW side of the Gebel El Zeit block, the basement carries three sub-orthogonal fracture sets (see also Fig. 3): cross-rift fractures form a northeasterly set with a vector mean strike and dip at 055°/79°, rift-parallel fractures form a northwesterly set with a vector mean at 315°/70°, and sheet fractures constitute a southeasterly set with a vector mean 140°/45° (the right-hand rule is followed throughout the paper) (Fig. 6). On the NE side of the fault block, and in the Nubia Sandstone, only the cross-rift and the rift-parallel sets exist. Except for a fourth fracture set at 025°/82°, fractures in the basement of the Esh El Mallaha block are similar to those found in basement on the SW side of the Gebel El Zeit. Table 1 summarizes the present-day and restored vector means of all fracture sets in the NE and SW sides of the Gebel El Zeit and Esh El Mallaha blocks.

All fracture sets in the basement were restored to their pre-Nubia datum by rotating the Gebel El Zeit block 42° (average dip of the Nubia Sandstone bedding) in a clockwise sense (looking NW) along an axis at 320° (Fig. 6). Fractures in the Nubia Sandstone were restored by rotating the block 35° along the same axis of rotation. The difference in the amount of rotation required to restore the basement (42°) and the Nubia Sandstone (35°) may indicate that the basement was tilted 7–10° prior to the deposition of the Nubia Sandstone, or that there was 7–10° of rotation between the formation of the basement and Nubia Sandstone joints. The restoration brings the 315°/70° and 055°/79° sets into a vertical attitude and the 140°/45° planes into a horizontal attitude. After restoration, only samples from the SW side of the Gebel El Zeit block and Esh El Mallaha block show a fracture set that restores to a horizontal attitude. The NW and ENE sets are found throughout the basement of the Gebel El Zeit and Esh El Mallaha blocks and the Nubia Sandstone but no fractures

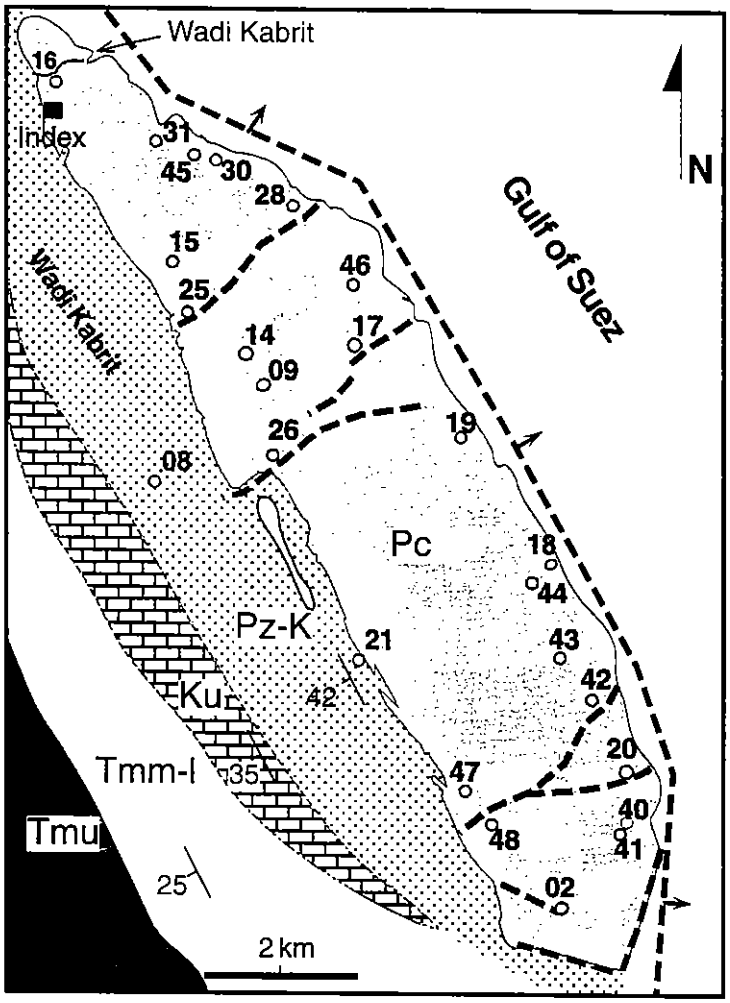

Fig. 5. A detailed map of the Gebel El Zeit main block. White circles represent the locations of measured scanlines. The solid black square is the station at which the 'background fracture spacing' is measured. Pc = Precambrian basement (granite). Pz-K = Nubia Sandstone, Ku = Cretaceous Matullah shales, sands and marls. Tmm-l = Lower Miocene, and Tmu = upper Miocene. Dashed lines are faults, and the arrows on the border fault show the dip direction. Many smaller faults were mapped within the block but are not shown for clarity. Wadi Kabrit is a strike-parallel valley formed by the erosion of the Nubia Sandstone along its contact with the basement.

were observed to continue from the basement into the Nubia Sandstone. The absence of a bedding-parallel fracture set (i.e. sheet) in the Nubia Sandstone indicates that it predates the Nubia whereas its absence on the NE side of the fault block reflects the limited depth at which the sheet fracture set formed.

Assessment of fracture distribution in a rock mass (e.g. a fault block) requires measurement of fracture orientation and spacing in outcrop or from well logs by two widely used methods: the scanline method (Terzaghi 1965; Priest & Hudson 1976; La Pointe 1980) and the area method (Davis 1984; Wu & Pollard 1995). The scanline method accounts for the angle between the scanline and measured fractures, and yields data such as median fracture spacing and fracture frequency. These data can be statistically analysed and extrapolated to other wells or fault blocks. The area method gives the fracture density within the rock mass and takes into account the length of the fracture in addition to its orientation. The fracture density is defined as 'the total surface area of fractures divided by the volume of the rock in three dimensions, or the total length of fracture traces divided by the surface area of rock exposures in two dimensions' (Rouleau & Gale 1985).

The term 'fracture frequency' is sometimes used indiscriminately to refer to fracture frequency of more than one set. In this paper, the term 'fracture frequency' is restricted to the ratio of the number of fractures in one set to the length of the scanline perpendicular to that set. The ratio of the number of fractures from all sets to the length of the scanline, regardless

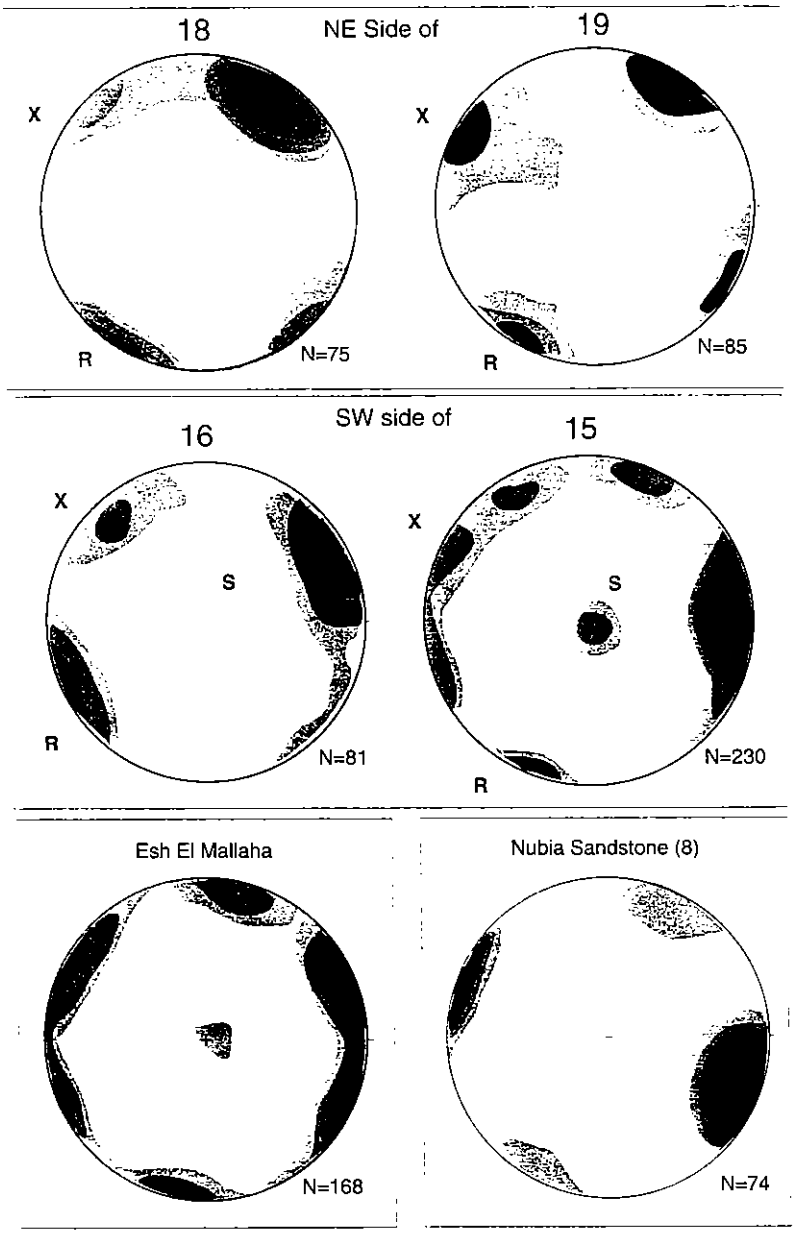

Fig. 6. Kamb contours of poles to restored fractures. Restoration is based on the average dip of the Nubia Sandstone (42°/230°). XR = cross-rift, RP = rift-parallel, and SF = sheet fractures. Only the SW side of Gebel El Zeit and Esh El Mallaha block show a fracture set that restores to horizontal. N = number of fractures. The number on the top of each diagram is the station number. Contour interval = 2 sigma.

of the orientation of the scanline, is referred to as the 'total fracture frequency'. Thus, this ratio may vary with the orientation of the scanline. Total fracture frequency is particularly useful when documenting fractures sampled by well logs. Fracture frequency may be a suitable description for uniformly developed fracture spacings; however, when the fracture spacing changes either gradually or abruptly, fracture frequency is not a suitable description for fracture development. If the fractures are well-developed, the total fracture frequency can be used as a qualitative measure of fracture density, especially when referring to a volume of rock (Wu & Pollard 1995).

In the Gebel El Zeit block, the cross-rift set is well-developed and has a uniform spacing (≤ 0.5 m) on both the SW and NE sides of the fault block (Fig. 7). On the other hand, the local spacing of the rift-parallel set shows an increase with distance from the fault: the spacing is a minimum (≤ 0.5 m) near the border fault, larger at the SW side of the block (0.3–1.15 m), and a maximum within the Esh El Mallaha

Table 1. *Present-day/restored vector means of fracture orientations in the Gebel EL Zeit and Esh El Mallaha fault blocks, Gulf of Suez*

Set/Area	NE GZ	SW GZ	EEM
RP or RP′	320/67 [301/88]	330/70 [335/88]	(055/88)
XR	56/78 [66/83]	45/77 [34/81]	(055/88)
SF	–	155/45 [158/2]	143/7
RP or RP′	320/67 [301/88]	330/70 [335/88]	325/85
NNE	(037/83)	(025/82)	026/88

Parentheses indicate that the fracture set is poorly developed in that area, and brackets enclose restored vector mean orientations. At least 200 fractures were used to determine the vector mean. NE GZ and SW GZ = northeast and southwest sides of the Gebel El Zeit block, respectively, and EEM = Esh El Mallaha fault block. XR = cross-rift fractures, SF = sheet fractures, RP = rift-parallel fractures, NNE = north-northeast fractures.

block (0.65–1.25 m). The NNE set within the Gebel El Zeit block has a local spacing that ranges from 0.9 m to 0.24 m whereas in the Esh El Mallaha block it averages 0.3 m. Sheet fractures have a local spacing that varies between 0.25 m at the top of the Esh El Mallaha block to 0.6–1.2 m in the SW side of the Gebel El Zeit block, but they are absent in the NE side. Sheet fractures and the distribution of their fracture frequency will be discussed in the next section.

In this paper, we distinguish between a local fracture spacing and a background spacing. The first is the median spacing for fractures of a single set at any site of interest. The second is the spacing measured at an arbitrary reference site (i.e. the index station in Fig. 5), some distance away from either faults or dykes. In a sense, this background spacing is a measure of fracture development in basement unaffected by local structures. By taking the ratio of the local spacing of a particular fracture set to its background spacing, we obtain a normalized fracture spacing that gives an indication of local fracture development.

In order to compare spacing data at different stations, we normalized the local fracture spacing using data from the index station (Table 2). Only vertical fracture sets are normalized because they occur throughout the granite blocks (horizontal fractures have background spacing equal to infinity, i.e. deep basement was not fractured in this orientation). Thus, a normalized spacing of 1 indicates that the local outcrop has a set of fractures spaced equivalent to the background fracture spacing. Therefore, if the normalized spacing is <1, the local fracture set is better developed, and if normalized spacing is >1, the local fracture set is less developed. In other words, if normalized spacing is <1, the local fracture frequency is high, whereas if normalized spacing >1, the local fracture frequency is low. Figure 8 shows that fracture development of the rift-parallel set in the NE side of the Gebel El Zeit block is twofold higher than in the SW side, and threefold higher than in the Esh El Mallaha block. Thus, the regional fracture frequency determined from scanline measured at the Gebel El Zeit and the Esh El Mallaha blocks changes regionally, according to location relative to the border fault.

Normalized fracture spacings in the Gebel El Zeit and Esh El Mallaha blocks not only show the degree of fracture development, but can also reflect the correlation between a fracture set and its relative age. This correlation stems from the observation that the first, or oldest, fracture set will tend to be more developed (i.e. longer, more closely and uniformly spaced, and higher in frequency) than the later, or younger, fracture sets. The decrease in fracture development is related to the heterogeneities in the stress field induced by the presence of older fractures. For example, the NNE, the youngest fracture set, is well-developed (background spacing = 0.6) in the Esh El Mallaha block but is less developed in the Gebel El Zeit block (background spacing = 1.29–1.54) whereas the cross-rift (ENE) set is best developed in the Gebel El Zeit block and least developed in the Esh El Mallaha block (Fig. 8). In summary, the older sets, cross-rift and rift-parallel, are well-developed in the Gebel El Zeit block, whereas the youngest set, NNE, is well-developed in the less-fractured, Esh El Mallaha block.

Factors affecting fracture spacing

Extension fractures develop in response to the tectonic stresses by propagating in the orientation of maximum horizontal stresses (Engelder & Geiser 1980). The extent (regional or local)

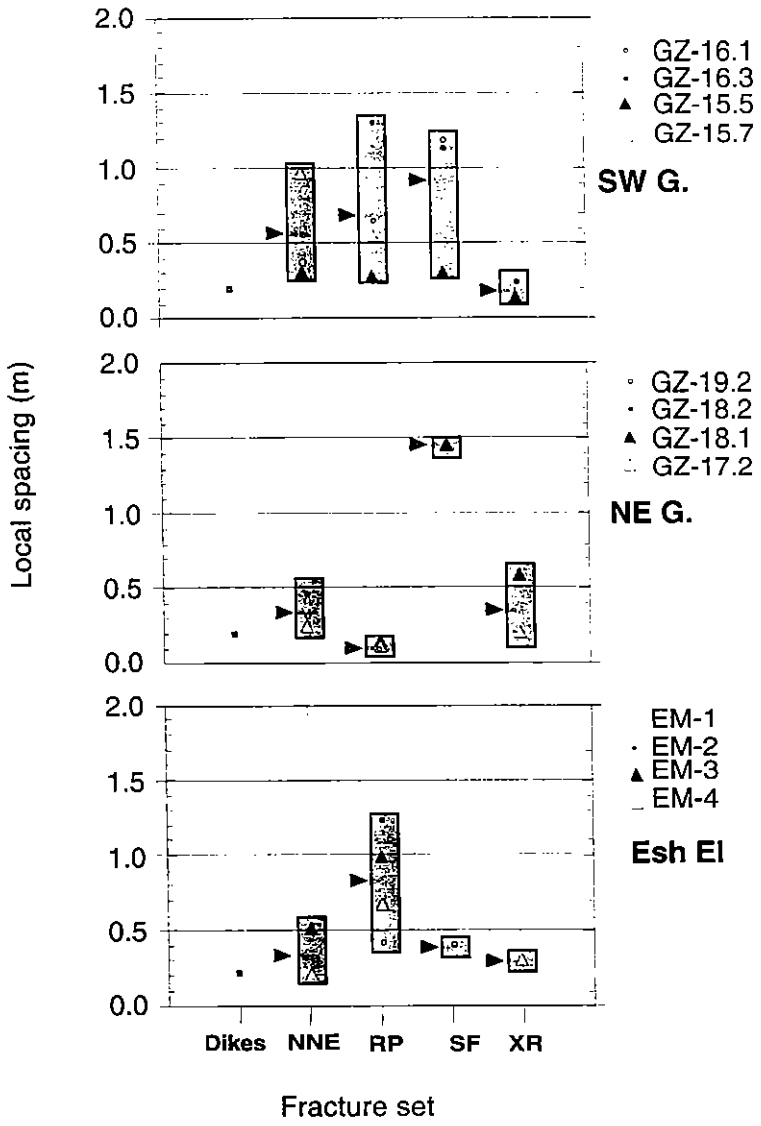

Fig. 7. Median spacing of fracture sets measured at different stations (legend on right) in the Gebel El Zeit (GZ) and Esh El Mallaha (EEM) blocks. The rift-parallel set has the smallest spacing near the border fault (NE side), and the largest spacing is recorded at the Esh El Mallaha block. Fracture spacing of dykes is plotted for comparison. RP = rift-parallel, XR = cross-rift, SF = sheet fractures, and NNE = north-northeast fractures. The small arrows to the left of the grey boxes marks the average of fracture spacings measured along different scanlines.

of the stress field, homogeneity of rock and its elastic properties all contribute to determining the intensity of fracturing in rock. For a particular rock type, the fracture spacing, as defined in the previous section, is rather uniform unless other local structures (e.g. faults) contribute to the deformation. This uniform spacing is thought to be controlled by stress shadows ranging from reduced crack-normal tensile stress in the vicinity of joints (Gross *et al.* 1995). A uniform fracture

Table 2. *Background spacing data used to normalize fracture spacing data at different stations*

Set	XR	SF	RP	NNE
Background spacing	0.34	–	0.66	0.44

Each number represents the median of the particular set spacing at the index station (see Fig. 5). Notation as in Table 1.

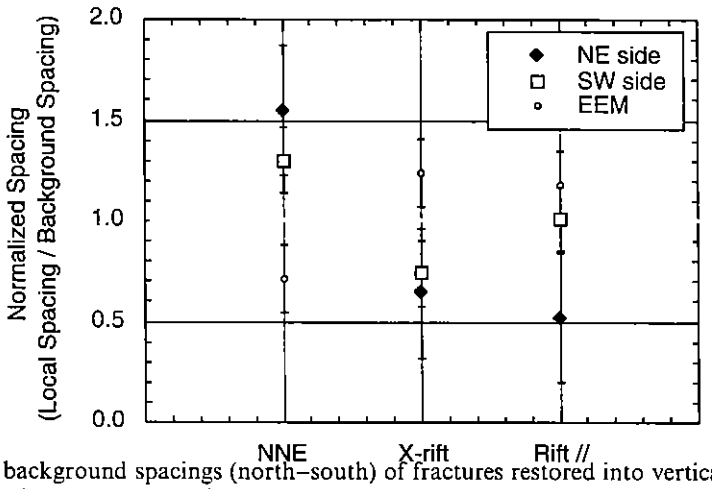

Fig. 8. Normalized background spacings (north–south) of fractures restored into vertical. The background spacing is defined in the text. A normalized spacing of 1 indicates that the fracture set has a 'normal' fracture spacing, while a normalized spacing greater than or less than 1 indicates that the fracture set is either poorly, or well developed respectively. The bars are one standard error from the mean. EEM = Esh El Mallaha block.

spacing implies that the fracture spacing is approximately constant along the scanline. Within the Gebel El Zeit and the Esh El Mallaha blocks, such uniformity in fracture spacing is not common. Fracture spacing of systematic sets varies from one set to the other, within a single set, and from one station to the other. Below, we discuss three processes that reduce the fracture spacing and, consequently, increase total fracture frequency (and density).

Sheet fracturing

Axial splitting is a process by which joints propagate parallel to the topographic surface as long, broad sheet fractures that reach up to 200 m in length (Nemat-Nasser & Horri 1982; Holzhausen 1989). Sheet fractures are well-developed in granitic rocks and sandstones (e.g. the Colorado Plateau), but are less common in mafic or other sedimentary rocks. Sheet fractures form as extension cracks having apertures of 1–2 mm and are likely to remain open because of surface asperities. Accordingly, sheet fractures permit fluid flow and will greatly enhance the interconnectivity of a fractured basement rock. We follow Holzhausen (1989) in making the distinction between sheet fractures and exfoliation fractures: the former are driven by non-thermal horizontal stresses, whereas the latter are driven by thermal stresses induced by annual or daily ambient temperature cycles.

In the Gebel El Zeit block, the sheet fracture set (140°/45°) is found on the SW side of the fault block but is almost absent on the NE side (Fig. 6). After restoring the Gebel El Zeit block to its pre-Nubia datum, the SW side becomes the top of the basement whereas the NE side rotates to a deeper portion of the basement (Fig. 9). Because the 'bedding-parallel' fractures on the SW side (top of basement) of the Gebel El Zeit block are restored to the horizontal and because they are rarely present on the NE side of the block, we interpret these as sheet fractures. The local fracture spacing of the sheet set gradually increases with depth from this contact with the Nubia Sandstone so that its fracture density decreases with depth (Fig. 10). Although these fractures are apparent as much as 40 m below the top of basement, outcrop limitations restricted our scanlines to 14 m. Data from subsurface fracture logs of the Ashrafi Field show that sheet fractures exist down to 150 m from the top of basement. In addition, very rare occurrences of sheet fractures are observed in the NE side of the Gebel El Zeit block which projects to 1.7 km below the top of basement. The behaviour of the sheet fractures within the Gebel El Zeit block resembles that of the Chelmsford Granite, New England, where Holzhausen (1989) and Jahns (1943) similarly observed a decreasing sheet-fracture frequency with depth.

Regionally, sheets between fractures at the top of basement in the Gulf of Suez become progressively thicker, from 0.2 m at Esh El Mallaha to 0.6–1.2 m SW of Gebel El Zeit. This pattern arises since Gebel El Zeit basement was uplifted approximately 150 Ma prior to Esh El Mallaha, therefore erosion exposed deeper and thicker sheets. Except for very rare occurrences, no sheet fractures were found to have a present-day horizontal attitude, or to be parallel to the

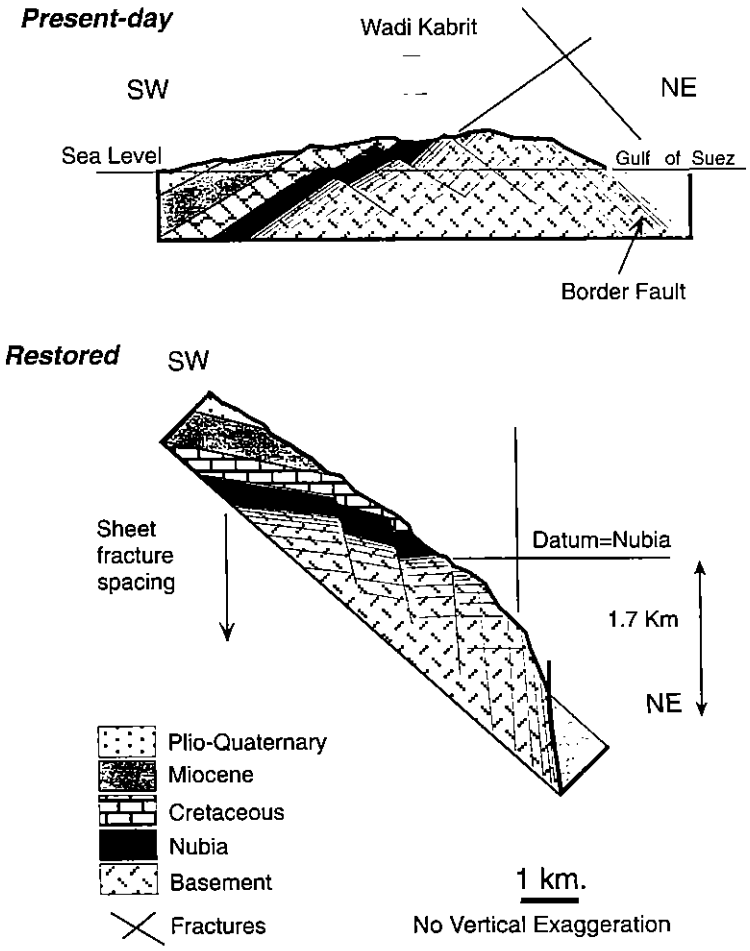

Fig. 9. A cross-section of Gebel El Zeit showing the restoration of basement rock on the SW side as the top of basement, while the NE side becomes a deeper basement.

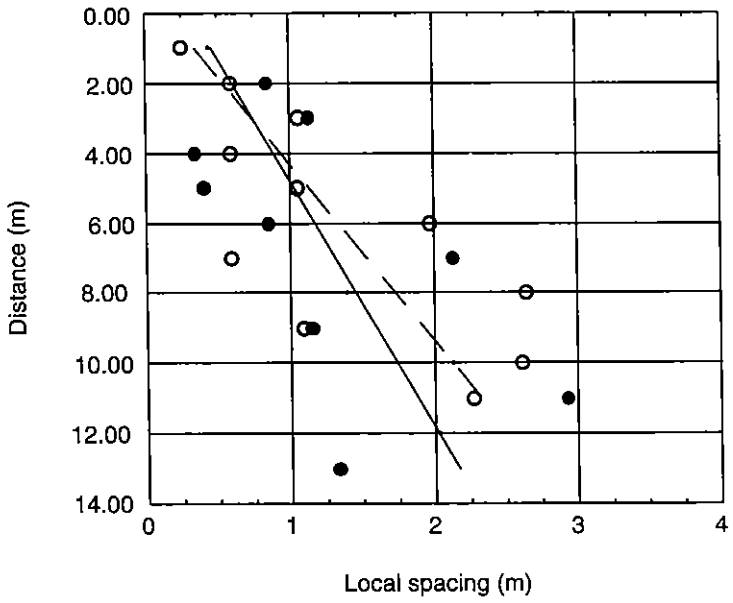

Fig. 10. Distribution of sheet fractures with depth as indicated by the data from two scanlines (solid and open dots). Solid and dashed lines are best fits of the two scanlines. Outcrop limitations restricted length of scanlines, but sheet fractures can be traced in some outcrops down to 40.0 m.

present-day topographic surface. Lack of post-Nubia sheet fractures is due to the intense fracturing of the basement which dissipates the stresses necessary to form large horizontal fractures.

Faulting

In the basement of the Gebel El Zeit and Esh El Mallaha blocks, faults strike parallel to the dominant ENE and NW fracture sets and mainly occur as dip-slip normal faults. These faults are commonly accompanied by features such as pinnate joints, tail cracks, mullions and tension gashes that are often lined or filled with vug-filling quartz. Although fracture spacing is rather uniform at a distance from faults, deviations from this uniformity occur near faults, particularly in footwalls (Fig. 11). The fracture spacing of a fault-parallel fracture set is usually less than 0.75 m but becomes much smaller in proximity to faults (Fig. 7). In other words, the fracture frequency, for example, of the rift-parallel set, gradually increases towards the border fault (Fig. 8). A similar behaviour is observed on a single-fault scale. Here, the fault-parallel fracture spacing decreases near individual cross-rift and rift-parallel faults (Fig. 12). In Fig. 12, the spacing data of a fault-parallel set are plotted against the distance from the fault. The data show that: (1) the frequency of a fault-parallel set increases near the fault; and (2) the rift-parallel fracture set has a higher fracture frequency than the cross-rift set at distances greater than 5 m from the fault.

In addition to the increase in the fracture frequency near faults, movement along faults

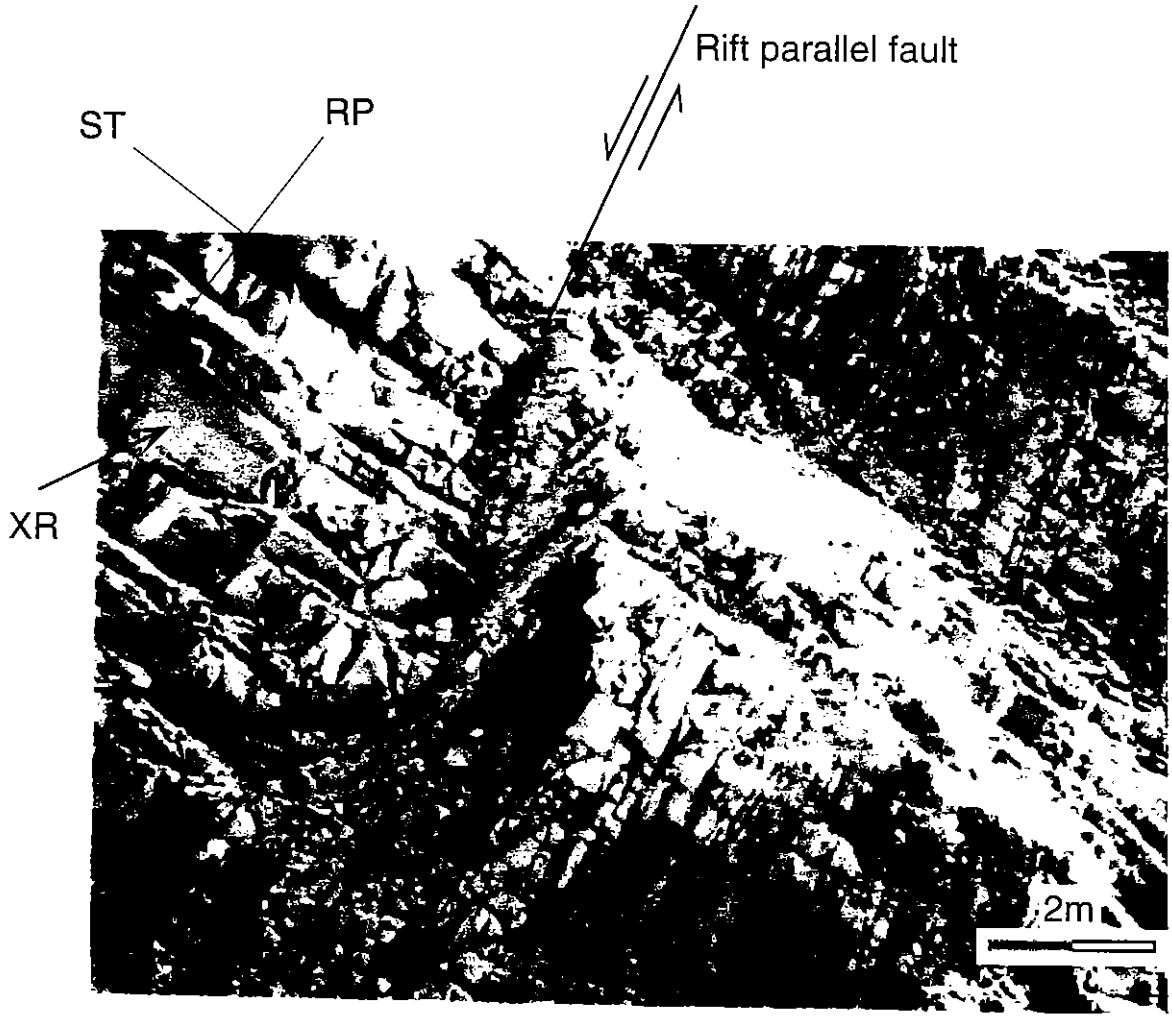

Fig. 11. Photograph of a rift-parallel fault in granite of the Gebel El Zeit block, looking SE. Wadi Kabrit is to the right of the photo. The fracture density near the fault is very high (compare to Fig. 3), especially in the footwall. Note the higher fracture density in the hangingwall within 1 m from fault surface. Fracture set symbols are as in Fig. 3.

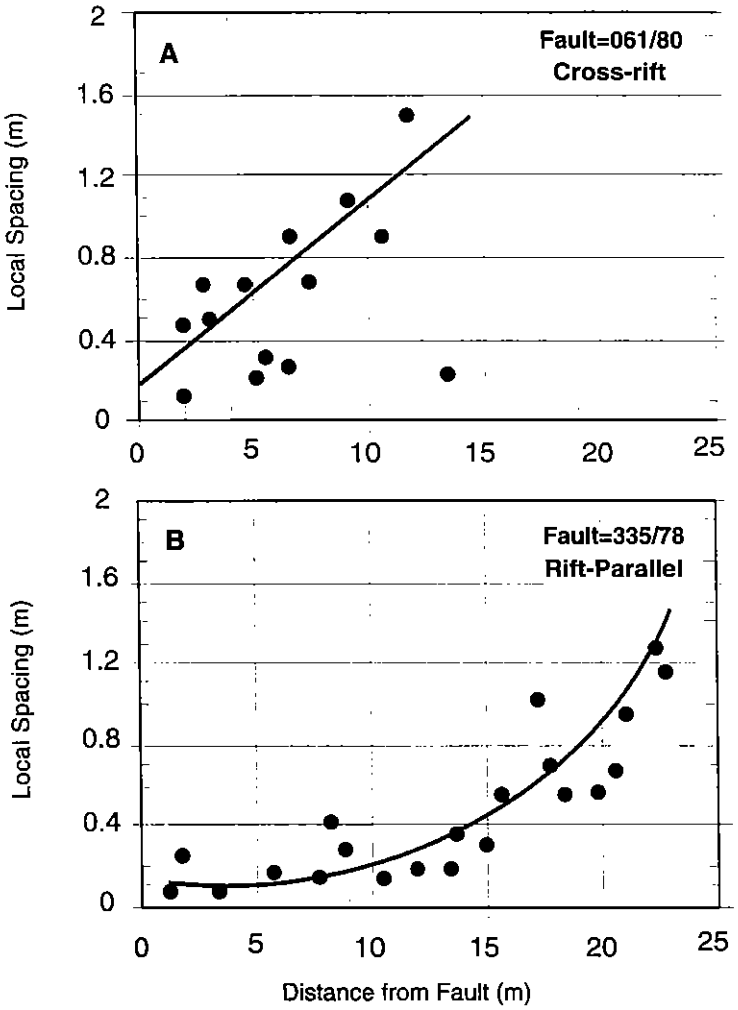

Fig. 12. Distribution of fracture spacing of fault-parallel fractures. Fracture spacing tends to increase with distance away from the fault. Cross-rift fractures tend to have a linear distribution (**A**) whereas rift-parallel fractures tend to have an exponential distribution (**B**).

causes block rotation and this may influence propagation of later fractures. The addition of fractures and block rotation leads to a larger scatter in fracture orientations so that fractures near faults plot as a girdle whereas those measured away from faults plot as well-clustered maxima (Fig. 13).

Dyke emplacement

Andesitic and rhyolitic dykes in the Gebel El Zeit block extend for distances of more than 500 m parallel to the ENE cross-rift faults and fractures. Sills strike parallel to the Gulf of Suez and dip to the SW parallel to the Nubia-basement contact. The small thickness (*c.* 1 m), weathering and infrequent occurrence limited field work on sills, hence the data presented here are for dykes only.

The fracture spacing within dykes averages approximately 0.18 m and thus leads to the highest fracture frequency anywhere in the Gebel El Zeit and Esh El Mallaha blocks. In a dyke, the majority of fractures strike parallel to the orientation of the dyke itself, implying that there is a genetic relationship between dykes and fractures (Fig. 14). In addition to their high internal fracture frequency, some dykes are bordered by a zone of dyke-parallel fractures that gradually become less frequent away from the dyke walls (Fig. 14). The adjacent zone is approximately equivalent to the dyke in thickness. Such fractured zones may be interpreted as a process zone ahead of the dyke tip (Delaney *et al.* 1986) or as a manifestation of thermal stresses developed in the host rock after dyke intrusion. Alternatively, this may be a zone of weakness that was exploited during the intrusion of the dyke.

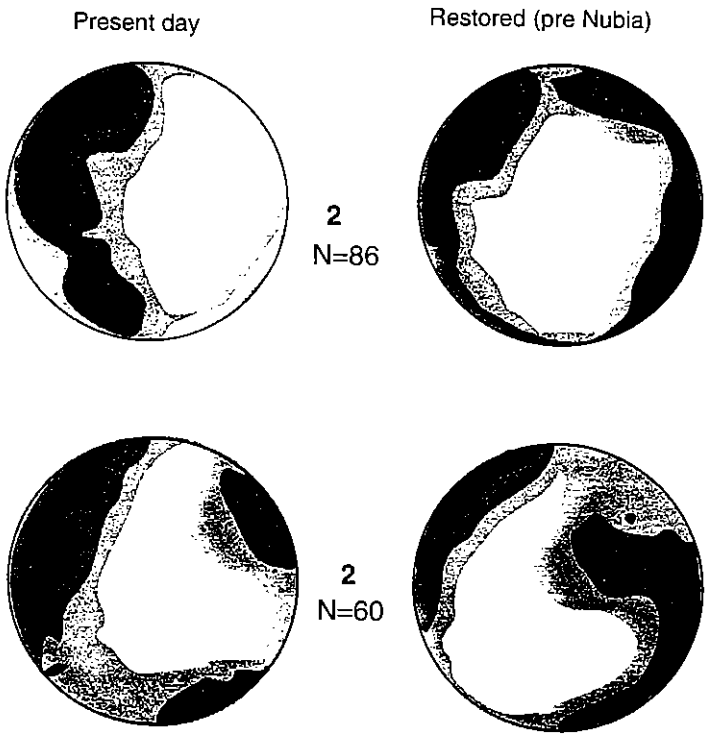

Fig. 13. Variation of fracture orientations in proximity of faults. Fractures plot on equal-area plots as a girdle instead of as well-defined maxima. Data from the NE and SW sides of Gebel El Zeit.

The Ashrafi Oil-field

The Ashrafi Oil-field (Fig. 1) is located within a series of southwesterly dipping fault blocks that were rotated along rift-parallel, NE-dipping faults. Composition of the cover and basement rocks, and structure of the Ashrafi Field resemble that of the Gebel El Zeit block. The basement is mainly granitic (alkali granites) and is intruded by andesitic and rhyolitic dykes. Well logs show that the basement is covered by pre-rift strata in some wells and by the post-rift Miocene clastics or evaporites in other wells. For example, the basement of wells A3 and C-1X is covered by the Nubia Sandstone whereas that of well B3 is covered by lower–middle Miocene clastics and evaporites (Fig. 15). The contact between the basement and the overlying sediments is defined by discontinuity in the gamma-ray and density logs. Dykes within the granite can also be resolved using the same logs.

Formation Micro Scanner (FMS) and Formation Micro Imager (FMI) data in the Ashrafi basement are available from several wells. The average total fracture frequency is calculated from corrected fracture orientations and plotted as a fracture density curve plot (FVDC) (Fig. 15). Similar to a scanline, the FVDC is calculated as the number of fractures recorded by the FMS tool per unit depth (an increase in frequency = a right shift in FVDC). Sub-surface fracture data from the Ashrafi Field show three dominant sets: a rift-parallel, cross- rift and sheet fracture sets similar to those in the Gebel El Zeit block. Fracture sets in the basement rocks of the Zeit Bay Field (Fig. 1) also resemble those in outcrop (Zahran & Ismail 1986). However, fracture attitudes may differ owing to the difference in the fault-block orientation or amount of block rotation.

The distribution of fracture density in the sub-surface varies according to the factors defined before (sheet fracturing, faulting, and dyke emplacement). In both the Ashrafi and Zeit Bay Fields (Fig. 1), the fracture density in the sub-surface shows an abrupt increase if the borehole intersects a dyke (Fig. 16). In addition, boreholes intersecting a rift-parallel fault, e.g. wells B2X, and A3, show two dominant fracture sets similar to the NE side of the Gebel El Zeit block. Furthermore, the fracture density in the basement of the Ashrafi Field shows a correlation between the presence or absence of pre-rift sediments and total fracture frequency indicated by the FVDC. Wells where the basement is overlain by the Nubia Sandstone, e.g. A3, show a higher total fracture frequency than those where the basement is overlain by the Miocene section, e.g. well B2X (Fig. 15).

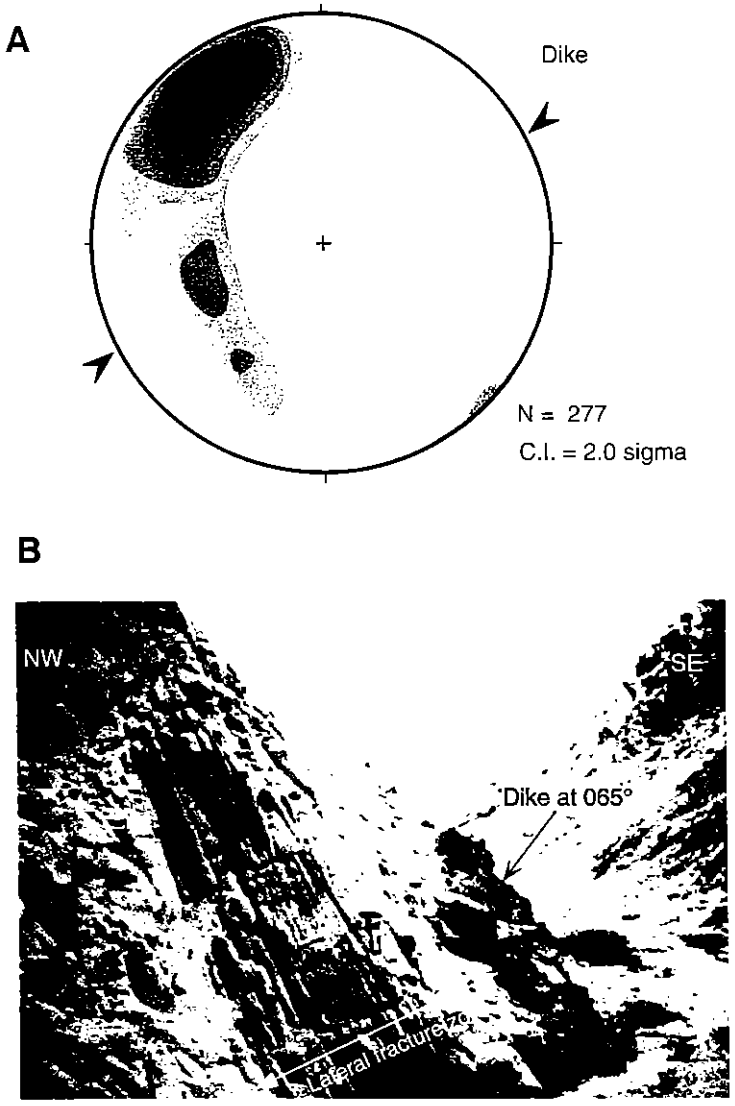

Fig. 14. (A) Kamb contour, and (B) field photograph of a fractured andesitic dyke exposed at the Gebel EL Zeit block. Most of the fractures within the dyke strike parallel to the dyke. In addition, dyke walls are fractured by a lateral fracture zone that, again, strikes parallel to the dyke. Note the areal extent of the dykes shown in the background of the photo.

In order to test this correlation between pre-rift sediments and fracture frequency, scatter diagrams of poles to fractures from the Nubia-covered A3 well and the Miocene-covered B2X well are compared in Fig. 17. In the top row, equal intervals of basement are compared but the A3 basement is deeper than the B2X. In the lower row, data from the bottom 25 m in both wells are compared. Fracture orientations in A3 are similar to the rift-parallel, cross-rift and sheet orientations of the Gebel El Zeit and Esh El Mallaha blocks. Although both wells show a decrease in fracture frequency with depth, the deeper interval of A3 has a higher fracture density than the shallower interval of B2X. In addition, sheet fractures are abundant in the A3 well but are almost absent in the B2X basement. This situation is similar to comparing the SW side of the Gebel El Zeit block (A3) with its NE side (B2X). The same relationships were observed for all the wells where the sheet fracture and total fracture frequency are higher in the first than in the second. In other words, basement rocks covered by pre-rift sediments (e.g. Nubia Sandstone) have a higher fracture density than those covered by syn- or post-rift sediments (e.g. Rudeis Formation). Therefore, the presence of pre-rift cover appears to preserve the fractured rock beneath it (especially sheet fractures) from erosion, while post-Nubia

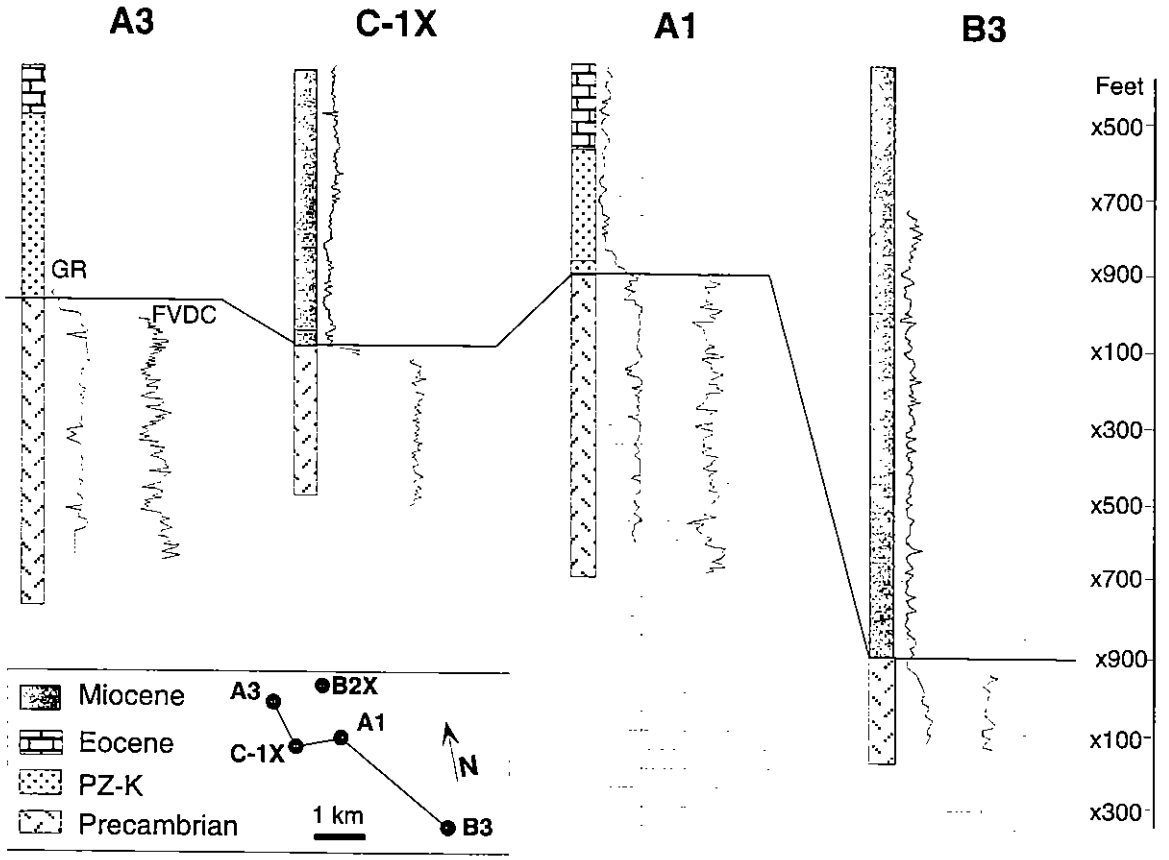

Fig. 15. Four well logs from the Ashrafi Field. The strike of the cross-section is NW, parallel to the Gulf of Suez. In terms of stratigraphy and structure, the A3 well is similar to the A1, A2, A5 and C-1X; and the B3 well is similar to the B2X and B1X. Grid is 50 ft intervals, GR is the gamma-ray log, and FVDC is the fracture frequency curve from FMS data. The FVDC shows an increase in the total fracture frequency if the curve shifts to the right, and vice versa. Log data modified from Deri (1993).

exhumation of the basement subjects it to erosion and loss of significant fracture density with the removal of rocks containing sheet fractures.

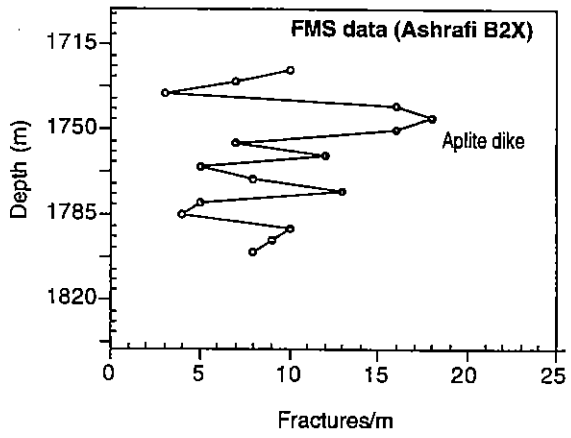

Fig. 16. Sub-surface example of increase in fracture density along zones intruded by dykes: Ashrafi B2X well.

The similarities of fracture orientation and distribution in sub-surface (Ashrafi and Zeit Bay) and surface (Gebel El Zeit and Esh El Mallaha) fault blocks justify the use of surface fault blocks as analogues for the sub-surface rocks. However, differences in fracture frequency as illustrated above (B2X versus A3) and the lack of strong 'stratigraphic markers' in the basement may lead to incorrect interpretations. For example, B2X was drilled near the crest of a rotated fault block, a customary target for drilling, yet the fracture density in the basement was low at this well.

In order to completely understand the fracture density distribution in basement, these fractures must be considered in a tectonic context. The style of uplift, proximity to block-bounding faults, the depth of erosion, and the interaction of more than one fracture set are important factors. Based on the tectonic style of the rift basin, the following section presents two models where fracture distribution differs according to the nature of the block uplift and erosion.

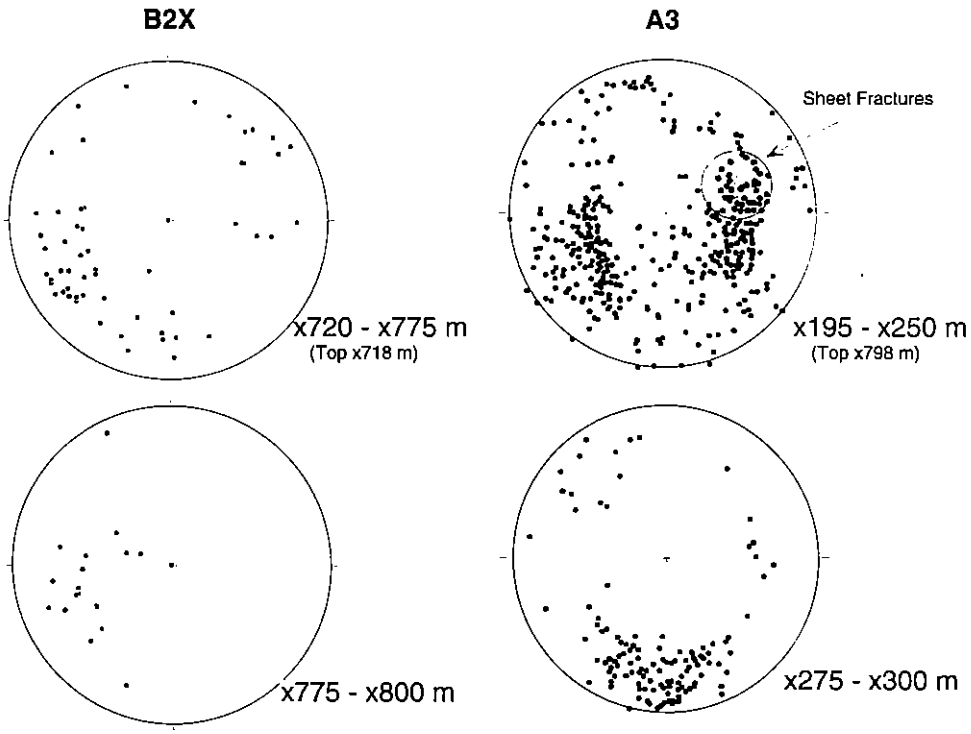

Fig. 17. Lower-hemisphere stereonet projections of poles to fractures in the Ashrafi B2X and A3 wells; sheet fractures plot in the eastern side of the stereo plot (shaded). The fracture density in both wells decreases with increasing depth, particularly sheet fractures in A3. The higher fracture density is present in the Nubia-covered A3 well while the lower fracture density is present in the Miocene-covered B2X well. The last 25 m of the A3 well were drilled through the youngest granite intrusion which was fractured under a different, more easterly compression than the older granites on top of it.

Discussion

Fracture distribution in faulted basement blocks

The local fracture density of a fault block is largely controlled by sheet fracturing, faulting, dyke emplacement and erosion. The term 'fracture density' is used here qualitatively to indicate those portions of a fault block which are more fractured than others. Except for erosion, the style of deformation (rifting) will control the location of maximum fracture density. We propose two models that illustrate this effect: a rotated-block model fitting the behaviour of the fault blocks exposed along the shoulders of the Gulf of Suez, and an uplifted-block model fitting the behaviour of the fault blocks off the southern coast of Vietnam (Khy 1986). Block rotation is typical for half grabens, whereas block uplift is typical for full grabens (Morley 1995).

Theoretically, fractures related to faulting dip at an acute angle to the fault surface, such as those presented in the block-uplift model (e.g. Hancock 1985). However, in the block-rotation model, rift-parallel fractures are modelled parallel to faults of that orientation as documented from field work. The discrepancy between the two models arises because faults in the Gebel El Zeit block were initiated utilizing previously existing rift-parallel fracture fabric, and consequently fractures and faults parallel each other (Younes 1996).

In the block-rotation model, we assumed the absence of post-rifting sheet fractures. This assumption is based on field data from the Gebel El Zeit block where occurrences of present-day sheet fractures are very rare. The lack of present-day sheet fractures may be attributed to the high fracture density of the fault block, which inhibits the formation of large, uniform fractures. Alteratively, sheet fractures are best developed when uplifted block has undergone peneplanation. Thus, the rugged topography of the fractured basement of the Gebel El Zeit block would relieve the horizontal stresses necessary to propagate sheet fractures. The abundance of pre-Nubia sheet fractures thus suggests some degree of peneplanation which has been documented from the non-conformable relationships between the lower Nubia Sandstone and the

underlying igneous rocks, and from textural and mineralogical data of the lower Palaeozoic rocks (Klitzsch & Squyres 1990).

Block-rotation model

Rotation of fault blocks along listric or planar faults is a common style of deformation in half grabens (e.g. the Gulf of Suez) and leads to the exhumation of the uplifted edge of the block. Large amounts of rotation, proximity of the rotation axis to a fault, and large block sizes cause larger amounts of uplift, and consequently greater depths of erosion into the basement. The effect of rotation and erosion on the fracture density of a fault block is illustrated by a cross-section of the Gebel El Zeit block (Fig. 18). The fracture frequency of the sheet fractures increases towards the top of the block whereas that of the fault-parallel fractures increases towards the block-bounding faults.

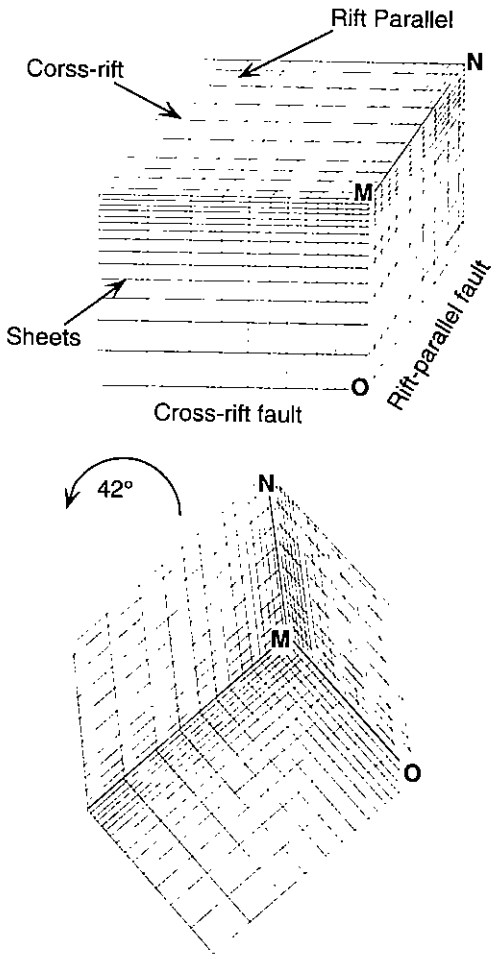

Fig. 18. Rotation of a fault block relocates the most fractured portion of a fault block as the crest of the block, MN. Subsequent erosion will strip off this part, leaving the block with lower fracture density. Point M is the most fractured portion of the block.

The intersection of three mutually perpendicular fracture sets localizes the fracture density along the edges of the block, and particularly towards a point where the three fracture sets intersect. Rotation and uplift of the fault block causes the uplifted edge to become the crest, where erosion will strip off rocks containing a high fracture density. A large amount of erosion will leave rocks of widely spaced fractures at the top of the basement (Fig. 19). Meanwhile, the graben receives sediments and will be filled, thereby protecting the underlying basement rock, with its relatively higher fracture density, from erosion. Because the frequency of sheet fractures gradually decreases with depth, higher fracture densities are found only where the basement cover was not deeply eroded. For example, the basement of the A3 well is overlain by the Nubia Sandstone, and thus shows higher fracture density largely because abundant sheet and rift-parallel fractures have not been exposed to erosion (Fig. 15). The Shoab Ali Field is located in the central Gulf of Suez, and is another example of a Nubia-covered basement producing field (Nagaty 1982). In contrast, the Ashrafi B2X block is a Miocene-covered, deeply eroded block and is not a basement producer.

Block-uplift model

Block uplift refers to a rifting style where the basement is faulted in a horst-and-graben style with little or no rotation. This style is typical in the central troughs of large rift basins and continental shelf margins (e.g. the Cuu Long (Mekong) and the Con Son rift basins, Vietnam; Chan *et al.* 1994). In contrast to block rotation, the block-uplift style differs in having smaller amounts of rotation and larger vertical displacements.

The model illustrated in Fig. 20 represents a horst uplifted along two sub-perpendicular faults with initial fracture density similar to that of Fig. 16, where fault-parallel fracture frequency gradually increases from the centre of the block towards the block edges. If the basement is exhumed, erosion will gradually remove the sheet fractures at the top while the graben will receive sediments from the eroded rocks. The removal of sheet fractures lowers the fracture density of the horst, while the sediment-filling of the graben protects the high fracture density in the underlying basement.

In this tectonic style, the maximum fracture density is localized at block-bounding fault

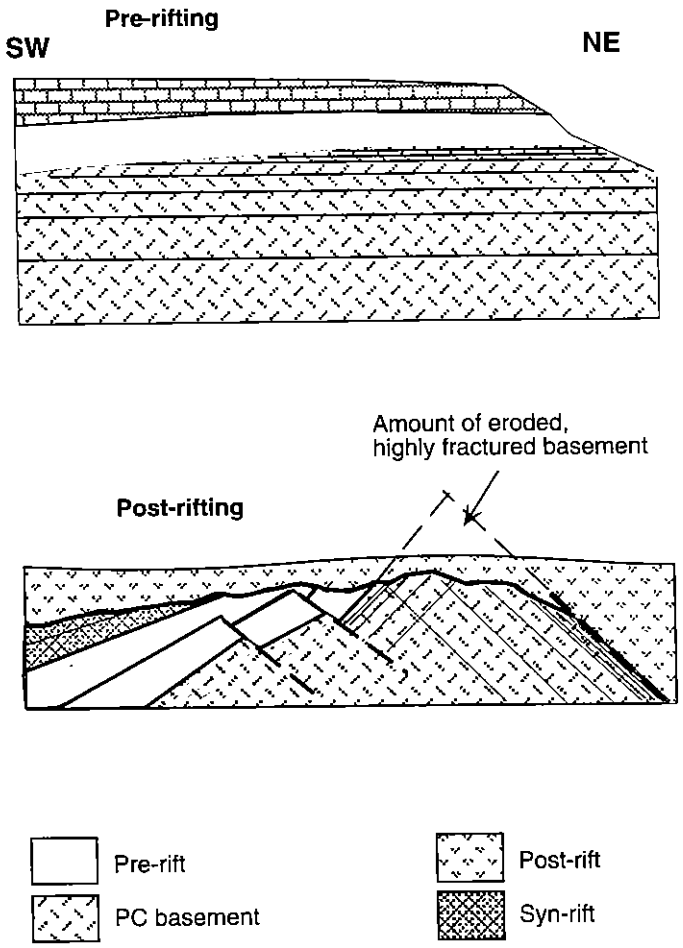

Fig. 19. Block-rotation model. The eroded basement crest is covered by post-rifting sediments (Middle and Upper Miocene) at the southern end of Gebel El Zeit. Dashed lines are faults and the NE fault is the border fault.

intersections (Fig. 20). The large vertical displacements on these faults (3–6 km; Chan *et al.* 1994; Arechev *et al.* 1992) reflect larger amounts of extension, and consequently larger fault-related fracture zones. In addition, the thick sedimentary column in the graben will allow lateral migration of oil from the source rock, or other reservoir rock, into the fractured basement. Thus, if the horst is eroded, fractures will be localized only at fault intersections, and there will be reduced chances for lateral oil migration, and hence oil accumulation in the horst block.

Alternatively, if the amount of uplift of a horst is insufficient to erode the entire sedimentary cover on top, the horst will have its highest fracture density at fault intersections and near the top of the block. In this case, penetrating the crest of a fractured basement reservoir block is recommended. Deep wells (4.5 km) penetrating over 1 km of fractured basement of the Cuu Long basin, Vietnam, could have intersected such large fault-intersection zones.

Where do fractured basement reservoirs occur?

In Fig. 21, we examine three possible fractured basement reservoir targets for each tectonic style as discussed above (Figs 19 and 20). Targeting the crest of the structure is routine in oil exploration; however, in fractured basement, crests are the most eroded. For example, well X was drilled on the crest of the structure in both tectonic styles where the basement is less fractured, and hence lower permeability values, such as those of B2X, are expected in both wells. Well Y, on the other hand, is drilled near fault intersections where fault-parallel fractures are well-developed and provide high permeability. Because well Y in the rotated block lacks sheet fracture intersections, it will show lower fracture density (and permeability) than an uplifted block. In addition, the decrease in the fracture density away from the fault will govern the 'thickness' of the reservoir in the

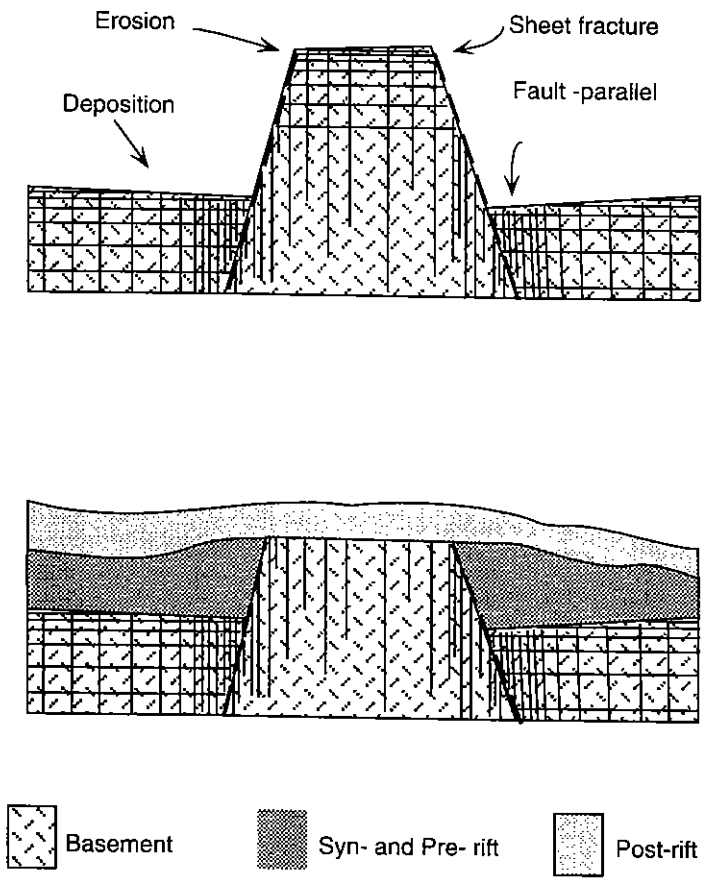

Fig. 20. Block-uplift model. Dashed lines are faults bounding the horst structure. Erosion of the horst will reduce the overall fracture density . Deposition of eroded material in the graben protects the basement's fracture density. The maximum fracture density occurs at fault intersections.

rotated block example, whereas the parallelism of the well bore to fractures in the uplifted block may be a disadvantage. Overall, well Y in block uplift is a better target than that in block rotation. Well Z is drilled in a highly fractured basement that is covered by pre- or syn-rift sediments where it is likely to encounter high fracture density in both wells. However, the well of the block-rotation model is a more promising target than that of the block-uplift model, simply because oil can migrate upwards through faults in the rotated block, but it is less likely that it will move laterally into the down-thrown block of the block-uplift model.

Other controls may influence the productivity of fractured basement rotated fault blocks. For example, some wells around the Ashrafi Field have fractured basement that is covered by the Nubia Sandstone. However, these wells were not basement producers simply because the fractured portions were below the oil–water contact, whereas the crests, the less fractured portion, were above it. Another situation arises if the fault and bedding attitudes inhibit the upward migration of oil into the fractured basement (e.g. if the fault and the beds dip in opposite directions). Despite these exceptions, fracture density within a basement fault block generally increases away from its eroded crest, and reaches a maximum below the uneroded portions.

Effect of fractures on permeability

Basement rocks, unless fractured, have very low permeability and porosity. Vertical fractures are generally abundant in basement rocks and provide conduits with high directional permeability and porosity. However, lateral communication may be reduced because of low fracture interconnectivity. Sheet fractures, with their large dimensions, can greatly enhance interconnectivity, especially at the top of basement. For example, basement in well A3, where high flow rates were recorded during production tests (28 BOPD/PSI on average), is highly fractured with an abundance of sheet fractures

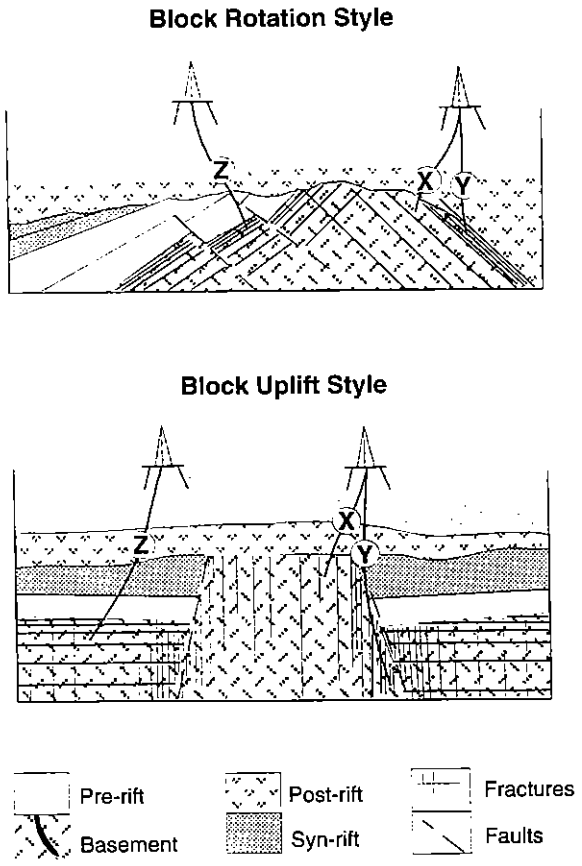

Fig. 21. Possible potential targets for fractured reservoirs. See text for discussion.

(Fig. 17). On the contrary, basement lacking sheet fracturing (e.g. B2X) is less permeable and porous as indicated by the low rates of production tests (4 BOPD/PSI). The extent, depth and distribution of sheet fractures is critical to the production of fractured basement reservoirs, particularly in fault blocks where the crest is eroded.

The presence of sheet and fault-related fractures is possibly the most significant factor in determining the quality of a fractured basement reservoir. Their presence localizes the fracture density at the edges of a fault block, and consequently creates potential high-permeability targets. In addition, the scatter of fracture orientations near faults increases the number of possible fracture intersections and hence the opportunity to develop a wellconnected fracture network that would increase the overall permeability.

Dyke geometry in the Gebel El Zeit block indicates that they were intruded through previously existing fractures. The high fracture density and the occurrence of lateral fracture zones marginal to dykes make them potential zones of high permeability. The strong parallelism of fractures within and around the dykes and the lower fracture density in the surrounding granite, could increase the permeability anisotropy. In Zeit Bay Field, such increases in permeability at dyke intersections are matched by an increase in production (Ismail & Abd-Elmoula 1992; Younes 1996).

Conclusions

Outcrop studies of the Gebel El Zeit and Esh El Mallaha blocks show that the fracture density of basement rocks increases by three geological processes: sheet fracturing, faulting and dyke emplacement. Sheet fracturing increases a block's fracture density near the top and provides the block with horizontal permeability. The continuous formation of sheet fractures depends on the intensity of fracturing of the block and may control the potential of reservoirs in uplifted blocks. Faulting is associated with veining and zones of higher fracture density that also increase rock permeability. In addition, fracture orientations show a wider scatter that may contribute to the increase of permeability near faults. Dykes have the highest fracture density, but the majority of these fractures strike parallel to the dyke orientation and thus may provide a path of permeability anisotropy. The existence of a dyke-parallel lateral fracture zone in the host rock will enhance this anisotropy.

Sub-surface studies in the Ashrafi Field show that rotation of a fault block relocates the highly fractured edge of the block as the crest of the block, whereas uplift of basement as a horst localizes the fracture density along the boundaries of the horst. In either mode of uplift, erosion will strip the rock of its highly fractured portions. Thus distribution of fracture density in a fault block depends on the depth of erosion, or the length of hiatus between the basement and the overlying cover. Fractured reservoirs are best-developed where the fractured basement was protected by the pre-rift cover and was not eroded.

Finally, the Gebel El Zeit and Esh El Mallaha fault blocks can be analogues to sub-surface Ashrafi blocks and outcrop characterization of fractures is necessary to properly evaluate fractured reservoirs.

This work was supported by a grant from Marathon Oil Co., Petroleum Technology Center. Logistical support was provided by Marathon Petroleum Egypt, Ltd. We greatly appreciate the efforts of Professor

Neil Hurley at Colorado School of Mines in pursuing the funds for this project and revising an earlier version of the manuscript. The authors wish to thank Adham Gouda, of Marathon Petroleum Egypt Ltd. for helping with the field work, and David Pollard and John Lorenz for helpful comments and review.

References

ALLAM, A. 1988. A lithostratigraphical and structural study on Gebel El-Zeit area, Gulf of Suez, Egypt. *Journal of African Earth Sciences*, 7, 933–944.

ARECHEV, E., DONG, T., SAN, N. & SHNIP, O. 1992. Reservoirs in fractured basement on the continental shelf of southern Vietnam. *Journal of Petroleum Geology*, **15**, 451–464.

BHATTACHARYYA, D. P. & DUNN, L. G. 1986. Sedimentologic evidence for repeated pre-Cenozoic vertical movements along the northeast margin of the Nubian Craton. *Journal of African Earth Sciences*, **5**, 147–153.

BOSWORTH, W. 1995. A high strain model for the southern Gulf of Suez (Egypt). *In*: LAMBIASE, J. J. (ed.) *Hydrocarbon Habitat in Rift Basins*. Geological Society, London Special Publication **80**, 75–102.

CHAN, T., HA, V., CARSTENS, H. & BERSTAD, S. 1994. Viet Nam, attractive plays in a new geological province. *Oil and Gas Journal*, **92**(11), 78–83.

COLLETTA, B., MORETTI, I., CHENET, P. Y., MULLER, C. & GERARD, P. 1986. The structure of the Gebel El Zeit area: A field example of tilted block crest in the Suez rift. *Eighth Egyptian General Petroleum Corporation Conference*, Cairo, November 1986.

DAVIS, G. 1984. *Structural Geology of Rocks and Regions*. Wiley, New York.

DELANEY, P. T., POLLARD, D. D., ZIONY, J. I. & MCKEE, E. H. 1986. Field relations between dikes and joints: Emplacement processes and paleostress analysis. *Journal of Geophysical Research*, **91**, 4920–4938.

DERI, S. 1993. *Structural Analysis of the Ashrafi Field, Gulf of Suez*. AGIP, internal report.

EL-SHAZLY, E., EL-KASSAS, I. & MOUSTAFA, M. 1979. Comparative fracture analysis and its relation to radioactivity in the pink granite of Um Had pluton, Central Eastern Desert, Egypt. *Egyptian Journal of Geology*, **23**, 95–110.

ENGELDER, T. 1982. Is there a genetic relationship between selected regional joints and contemporary stress within the lithosphere of North America?, *Tectonics*, **1**, 161–177.

—— & GEISER, P. 1980. Use of joints as paleostress indicators. *Journal of Geophysical Research*, **85**, 6319–6341.

FREEZE, R. & CHERRY, J. 1987. *Hydrogeology*. McGraw Hill, New York.

GREENBERG, J. K. 1981. Characteristics and origin of Egyptian Younger Granites: Summary. *Geological Society of America Bulletin*, **92**, 749–840.

GROSS, M., FISCHER, M., ENGELDER, T. & GREENFIELD, R. 1995. Factors controlling joint spacing in interbedded sedimentary rocks: integrating numerical models with field observations from the Monterey Formation, USA. *In*: AMEEN, M. (ed.) *Fractography: Fracture Topography as a Tool in Fracture Mechanics and Stress Analysis*. Geological Society, London, Special Publication **92**, 215–233.

HANCOCK, P. L. 1985. Brittle microtectonics: Principles and practice. *Journal of Structural Geology*, **7**, 437–457.

HEATH, M. 1985. Geological control of fracture permeability in Carnmenellis granite, Cornwall: implications for radionuclide migration. *Mineralogical Magazine*, **49**, 233–244.

HOLZHAUSEN, G. 1989. Origin of sheet structures: 1. Morphology and boundary conditions. *Engineering Geology*, **27**, 225–278.

HUANG, Q. & ANGELIE, J. 1985. Fracture spacing and its relation to bed thickness. *Geological Magazine*, **126**, 355–362.

HUSSEINI, M. I. 1988. The Arabian infracambrian extensional system. *Tectonophysics*, **148**, 93–103.

ISMAIL, F. & ABD-ELMOULA, I. 1992. The impact of dyke and brecciated zones on production from fractured basement reservoir of Zeit Bay field, Gulf of Suez, Egypt. *Egyptian General Petroleum Corporation Twelfth Exploration and Production Conference*, Cairo, November 1992.

JAHNS, R. 1943. Sheet structure in granites: Its origin and use as a measure of glacial erosion in New England. *Journal of Geology*, **LI**, 71–98.

KHY, L. 1986. The Structure of the Mekong trough. *International Geological Review*, **28**, 87–95.

KLITZSCH, E. & SQUYRES, C. H. 1990. Paleozoic and Mesozoic geologic history of Northeastern Africa based upon new interpretation of Nubia strata. *AAPG Bulletin*, **74**, 1203–1211.

LA POINTE, P. 1980. Analysis of the spatial variation in rock mass properties through geostatistics. *Proceedings of the 21st US Rock Mechanics Symposium*, 570–580.

MORLEY, C. K. 1995. Developments in the structural geology of rifts over the last decade and their impact on hydrocarbon exploration. In: LAMBIASE, J. J. (ed.) *Hydrocarbon Habitat in Rift Basins*. Geological Society, London, Special Publication **80**, 5–17.

——, NELSON, R. A., PATTON, T. L. & MUNN, S. G. 1990. Transfer zones in the east African rift system and their relevance to hydrocarbon exploration in rifts. *AAPG Bulletin*, **74**, 1234–1253.

MOUSTAFA, A. M. 1976. Block faulting of the Gulf of Suez. *Fifth Egyptian General Petroleum Corporation Exploration Seminar*, Cairo, 1–19.

NAGATY, M. 1982. The seven reservoirs of the Shoab Ali field. *Sixth Egyptian General Petroleum Corporation Exploration Seminar*, Cairo.

NELSON, R. 1985. *Geologic Analysis of Naturally Fractured Reservoirs*. Gulf.

NEMAT-NASSER, S. & HORII, H. 1982. Compression-induced nonplanar crack extension with application to splitting, exfoliation, and rockburst. *Journal of Geophysical Research*, **87**, 6805–6821.

OMAR, G. I., STECKLER, M. S., BUCK, W. R. & KOHN, B. P. 1989. Fission-track analysis of basement apatites at the western margin of the Gulf of Suez rift, Egypt: evidence for synchronoeity of uplift and subsidence. *Earth and Planetary Science Letters*, **94**, 316–328.

PATTON, T. L., MOUSTAFA, A. R., NELSON, R. A. & ABDINE, S. A. 1994. Tectonic evolution of the Suez rift. In: LANDON, S. M. *Interior Rift Basins*. AAPG Memoir, **59**, 9–55.

PERRY, S. K. 1983. *The Geology of the Gebel El Zeit Region, Gulf of Suez, Egypt*. University of South Carolina, Earth Science Resources Institute.

PETIT, J. P. 1987. Criteria for the sense of movement on fault surfaces in brittle rocks. *Journal of Structural Geology*, **9**, 597–608.

PRAT, P., MONTENEANT, C., OTT D' ESTEVOU, P. & BOLZE, J. 1986. La marge occidentale du Golfe de Suez d'apres l'etude des Gebels Zeit et Mellaha. *Documents et Travaux Institut Geologique Albert de Lapparent*, **10**, 45–74.

PRICE, N. J. & COSGROVE, J. W. 1994. *Analysis of Geological Structures*. Cambridge University Press.

PRIEST, S. D. & HUDSON, J. A. 1976. Discontinuity spacings in rock. *International Journal of Rock Mechanics and Mining Science and Geomechanics Abstracts*, **13**, 135–148.

ROULEAU, A. & GALE, J. E. 1985. Statistical characterization of the fracture system in the Stripa granite, Sweden. *International Journal of Rock Mechanics and Mining Science and Geomechanics Abstracts*, **22**, 353–367.

SCHURMANN, H. M. E. 1966. *The Pre-Cambrian along the Gulf of Suez and the northern part of the Red Sea*. E. J. Brill, Leiden.

STERN, R. J. & HEDGE, C. E. 1985. Geochronological and isotopic constrains on late Precambrian crustal evolution in the Eastern Desert of Egypt. *American Journal of Science*, **258**, 97–127.

—— & MENTON, W. I. 1987. Age of Fieran basement rocks, Sinai: implications for late Precambrian crustal evolution in the northern Arabian-Nubian shield. *Journal of the Geological Society, London*, **144**, 569–575.

STERN, R. J., GOTTFRIED, D. & HEDGE, C. E. 1984. Late Precambrian rifting and crustal evolution in the Northeastern Desert of Egypt. *Geology*, **12**, 168–172.

TERZAGHI, R. D. 1965. Sources of error in joint surveys. *Geotechnique*, **15**, 287–304.

WU, H. & POLLARD, D. D. 1995. An experimental study of the relationship between joint spacing and layer thickness. *Journal of Structural Geology*, **17**, 887–905.

YOUNES, A. I. 1996. *Fracture distribution in faulted basement blocks, Gulf of Suez, Egypt: Reservoir characterization and tectonic implications*. PhD thesis, Pennsylvania State University.

ZAHRAN, I. & ISMAIL, F. 1986. Similarity in composition and tectonic style between basement exposed in Gebel El Zeit and Zeit Bay subsurface. *Proceedings of the Eighth Egyptian General Petroleum Corporation Special Exploration Conference*, Cairo, November 1986, 183–205.